Crystallization Phenomenon of Zirconium Molybdate Hydrate to Prevent Encrustation

モリブデン酸ジルコニウム水和物の晶析現象とスケーリング防止

February 2014

Liang ZHANG

張　亮

Crystallization Phenomenon of Zirconium Molybdate Hydrate to Prevent Encrustation

モリブデン酸ジルコニウム水和物の晶析現象とスケーリング防止

February 2014

Waseda University

Graduate School of Advanced Science and Engineering

Department of Applied Chemistry, Research on Chemical Engineering

Liang ZHANG

張　亮

JUDGING COMMITTEE

Reference in chief

Waseda University Prof.Dr.Izumi Hirasawa

Referees

Waseda University Prof.Dr.Suguru Noda

Martin-Luther-University Halle-Witenberg Prof.Dr. Joachim Ulrich

CONTENT

Chapter1

Introduction

1.1 Energy Problem

Currently, ninety percent of the energy comes from fossil fuels, such as oil and coal. From now on, it is estimated that oil can meet the human needs for 41 years, gas for 63 years and coal for 212 years. It is uncertain whether new oil fields can be found in the next hundreds of years. Among the top 7 developed countries (Japan, UK, US, Canada, France, Germany and Italy), only UK and Canada can meet their energy needs by themselves. Although the fuel for nuclear power uranium can only be used for 72 years, it is estimated that uranium extracted from it can be used for hundreds of years nuclear fuel can be recycled. Energy consumption has been increasing with the development of technology. In fact, human beings are consuming two times as much as 100 years ago every day.

In the world, Japan, the US and Europe have 17.6% of the total population, while they are consuming about 56.3% of the energy. There are almost no energy resources in Japan, for example self-sufficiency rate of energy in 1999 is about 19%. Among the top 7 developed countries, the energy self-sufficiency rate of Japan is the second lowest, just ahead of Italy. Actually, the self-sufficiency rate is only 6% when deducting the contribution of nuclear power. Especially, 50% of the energy resources are oil, among which 87% come from politically turbulent Middle East. As a consequence, when oil crisis happens, energy supply will be unreliable.

There are almost no energy resources in Japan, for example self-sufficiency rate of energy in 1999 is about 19%. Among the top 7 developed countries, the energy self-sufficiency rate of Japan is the second lowest, just ahead of Italy. Actually, the self-sufficiency rate is only 6% when deducting the contribution of nuclear power. Especially, 50% of the energy resources are oil, among which 87% come from politically turbulent Middle East. As a consequence, when oil crisis happens, energy supply will be unreliable.

Japan is producing electricity from various methods to create the most applicable combination called best mix. In the 1970s, about 60% of the electrical power came from cheap and abundant oil. However, after two times oil crisis, excessive dependence on oil power became dangerous. With the oil price increasing, electricity fee was also rising. Insufficient oil supply became a basic reason for black out. After that, Japan began to introduce and develop nuclear power and natural gas as alternatives to oil. In regard to nuclear power, Japan made long-term and stable importing contract

for uranium with several countries. Different from renewables such as solar power and wind power, nuclear power is relatively cheap and stable, and thus became the most applicable base for electricity supply.

As the basis, nuclear power is working with the combination of thermal power produced from oil, coal and natural gas, etc. Moreover, during power peak, pumped-storage hydroelectric power is also introduced into the combination to become the best mix. In Asia, energy consumption is rapidly increasing while the dependence for oil is continuously rising. It is high necessary to take actions for global warming. Consequently, clean and energy-saving resources are under research, which are called new energies.

1.1.1 Solar Power

The energy from sunlight can be converted into electric power. Solar power has some merits, such as unexhausted and clean, while its efficiency is low and it cannot work under bad weather. In Japan, 2.09 GW solar power is installed in 1999, which is No.1 in the world at that time. Until 2010, solar power is estimated to be 48.2 GW, which is 23 times as much as 1999. Since solar power is not stable for electricity supply, it cannot serve as basic power source. In this regard, solar power is promisingly to be installed on the roof of factories and buildings as small power sources. [1-2]

1.1.2 Wind Power

Wind turbine can convert wind energy into electric power in the wind. Similar to solar power, wind power is also unexhausted and clean, but unstable because it depends on wind direction and velocity. Until the end of 2001, 2 GW wind power had been installed in Japan, but the data is estimated to be 30 GW by 2010. Considering the serious geographical conditions, although wind power is installed in all the possible places, it can only reach 92 GW (1% of the current electric power supply). [3]

1.1.3 Waste power generation

Combustible waste such as paper, wood and garbage can be used to generate electricity through heating steam. This system is called waste is called waste generation. 1999, waste-incineration power generation system in Japan generated about 900,000 kilowatts electric power in total from 171 bases, and the value is expected to reach five million kilowatts in 2010.

1.1.4 Fuel Cell

In fuel cell, electric energy can be obtained for the process that the hydrogen from fuel such as natural gas and oxygen from air act with each other and electrolysis of water. The energy efficiency of fuel cell can reach 60% while that of thermal power is only about 40%. Considering that fuel cell has high efficiency, less air pollution substance and noise, it will be the most applicable alternative to thermal power. [4-6]

1.1.5 Nuclear Fusion Generation

A large amount of energy will release when light nuclei, such as hydrogen and its isotope (tritium deuterium), confuse under ultra-high temperature and ultra-high pressure. Nuclear fusion generation system uses the same mechanism to generate energy just like what happen inside the sun. Deuterium and tritium can be obtained from seawater as fuel. This can be regarded as clear energy with no release of CO2, nitrogen compounds or sulfur compounds, which is usually generated due to the burning of fossil fuel and become the main cause of global warming. Also there is no need to worry about the high-level radioactive waste, which is the by-product of nuclear fission reactor.

In addition, the crystal methane ice-like consisting of a methane gas molecules and water molecules and expected biomass to make the gas as a source of energy by fermenting and plants of the United States, sugar cane, eucalyptus and other aqueous plants, etc., and new resources such as co-generation is a system that also use such as waste heat, which has been wasted until now when you produce and high trade, energy or been studied, you have or are used. [7-8]

1.2 Safety Measures for Nuclear Power

In reactor, nuclear fission increases, while natural fission becomes less. For safe operation in nuclear power plant equipment, the following three points will be considered.

Facilities cannot operate abnormally. Abnormal situation cannot develop into disasters. Radioactive substance cannot fly off when accident happens.

The facilities are capable to suffer unpredictable force, operation mistake by the operator and can maintain in safe condition when something unexpected occur. Operation of nuclear power plants is managed from the central control room for 24 hours. Chief operators in the control room are selected from those who pass the national exam and other operators are also asked to pass a strict training program.

Moreover, the alarm device, various sensors for early detection as well as an emergency stop device can stop reactor automatically when emergency is detected are also equipped.

Pellet, cladding, reactor pressure vessel, the containment vessel, the reactor building are the "quintuple wall" which keep the radioactive material inside. In addition, if accident happens in reactor, water can be sent to the "emergency core cooling system (ECCS)". Based on these measures, radioactive materials cannot be emitted out of the facility even in the case of accidents.

It is of great significance for nuclear plant to make comprehensive countermeasures for earthquake、typhoon, storm surge, tsunami, etc. Taking earthquake for an example, when constructing nuclear power plant, it is necessary to investigate the reason for earthquake in the construction site and build plants where rock shaking is slight during earthquake and the foundation is solid.

In a nuclear power plant history all over the world, some accidents have cause severe concerns on security. In order to prevent the accident in the future, it is important to learn a lesson from those accidents that happened before.

1.2.1 US Three Mile Island Nuclear Accident

On March 28th in 1979, radioactive substance flew off from reactor number two in US Three Mile Power Plant and the residents nearby had to refuge. Part of the residents living nearby had to evacuate though the quantity of the leaked radioactive material was small and had no affects on residents or animals. However the fuel in a nuclear reactor was damaged and it was just before meltdown. The cause of the accident was the defect of a design, the wrong operation, and the inappropriate react from the operators who noticed the abnormal situation. The accident showed people that meltdown was not a story that only happen in the movie "China Syndrome", it actually happened in real world and people who were in response of the industry should take action to work out a countermeasure. In Japan, strengthen of training program for operators and improvement of equipment had been made as a lesson learned from this accident.

1.2.2 USSR Chernobyl Accident

On April 26th in 1986, reactor number four in USSR Chernobyl nuclear power station exploded and radioactive substance flew off, which leaded to the most serious accident in nuclear power history. The radioactive substance firstly spread to Europe and all the world seriously suffered from this

disaster. Due to this miserable accident, 31 people died and about 135,000 residents had to move in order to refuge. This accident is caused by a series of reasons: output is likely to rise rapidly due to serious safety defects in design; there is no containment to prevent the radioactive substance; operators are lack of knowledge; failure to obey the rules; management system is not complete. From this accident, the concept of "safety culture" is widely proposed.

After learning the lessons from this accident, Japan decided to enhance nuclear disaster prevention measures and fostering safety awareness. In this way, promotion of safety research can be achieved. Furthermore, Japan's nuclear power plant is developing safety actions against the increasing nuclear accidents and adjusting its management system to avoid serious situations like the Chernobyl accident. Also, there is containment vessel for the nuclear reactor in Japan, so in case radioactive material leaked from the reactor, it can still be kept inside the facilities.

1.2.3 The Prototype Fast Breeder Reactor "Monju" Accident

On Dec 8th in 1995, 12/8/1995, in the prototype fast breeder reactor "monju" of power reactor in Tsuruga-Shi, Fukui, which belongs to the Nuclear Fuel Development Corporation (currently, Japan Atomic Energy Research Institute), liquid sodium disclosed from the secondary cooling system. Leaking sodium reacted with air to burn, and part of the sodium released through the ventilation system facilities.

1.3 Aqueous Reprocessing Method (Purex method)

By the Purex method, mixture of hydrocarbon diluent and tributyl phosphate (TBP) is used to extract the plutonium nitrate tetravalent and uranyl nitrate from nitric acid solution. This method was devised in 1949 based on the discovery that Warf [W2] could separate the tetravalent nitrate cerium from the rare earth nitrate by extraction using TBP, and was developed by the Knolls nuclear laboratory of General Electric. The examination of the pilot scale was done in Oak Ridge National Research Institute from 1950 to 1952. This method was adopted in the Savannah River plutonium production plant built in Aiken South Carolina by EIdupont de Nemours Inc. for USZEC, and Purex method of full-scale began operation in November 1954. Because of the success in this factory, redox method, which had been used by the General Electric Company under the Hanford plant, was be replaced by the Purex process in January 1956. The method was also used in the in re-processing

plant owned b Nuclear Fuel Service, which is operated in the West Valley, New York from 1966 to 1972. The plant is designed to reprocess 1MT of irradiated low-enriched uranium fuel per day, but the plutonium fuel and thorium fuel could also be reprocessed if the flow sheet was appropriately modified. The plant was noticed as the only factory in the United States that could reprocess the fuel from the private nuclear power plant sector. [9-11]

West Valley plant could satisfy the requirements of environmental protection or safety at the beginning, but the regulatory requirements on earthquake resistance and allowed release of radioactive waste became severely strict after 1970s. The construction of facility that converts plutonium nitrate into oxide, and solidify the pro solution with a high level which has been stored as a neutralized liquid was also requested. A great cost was needed to modify the factory in accordance with the request, and also the process capacity of this plant was small comparing to large-scale reprocessing plant under construction by Allied-General Nuclear Service. In 1976 West Valley plant had to shut down permanently. [12-14]

1.4 NEXT method

The NEXT process as illustrated in Figure 2.l is an advanced reprocessing based on the well established aqueous reprocessing with adaption Atomic innovative technologies in order to realize recycle as well as economical process. In this system, a wrapper tubing of a spent FBR fuel assembly is firstly remobed in a head end process, fuel pin bundle is sheared and then fuel meat will be dissolbed into nitric acid solution in a continuo dissolber. Excess amount or uranium required for producing core fuel will then be recovered by uranium crystallization method. This method has a simple principle and we are able to recover uranium as uranyl nitrate hezahydrate crystal by controlling the temperature of the solution without adding new reagent so that a simple reprocessing process would be realized. At a typical core condition, about seventy percent of uranium is required to be recovered from dissolver solution in order to make the ratio of residual uranium to plutonium in the solution almost equivalent to the composition in the core fuel. [15]

Next step is recovering Pu together with U and neptunium with separating most fission product elements by the well established solvent extraction method. A centrifugal contactor which has advantages will be utilized as the extraction equipment. Minor actinide elements such as Am and Cm

will be recovered with use of extraction chromatography from the raffeinate of cooptation.

Figure 2.1 shows the schematic flow of the NEXT process. Compared with the conventional PUREX process, crystallization and SEIFICS/JRUEX are added, and on the other hand, partitioning of Pu and purification of U and Pu are removed. After dissolving the spent fuels in the continuous rotary dissolver, NOx is blown through the dissolver solution to remove iodine. Blowing the NOx through the dissolver solution also benefits the controlling the valence of Pu. Moreover, concentration of the dissolver solution is expected by mixing the solution by NOx. In this design study, concentration of U is 500gU/l in the dissolver solution prior to the crystallization process. Partial separation of U in the crystallization process reduces the amount of aqueous and organic solutions processed in the following extraction process. U, Pu and Np are co-extracted and co-stripped in a single cycle using centrifugal contactors. Processing speed increases and the equipment gets compact by using centrifugal contactors in the extraction process. The number of equipment is reduced by removing partitioning of Pu and purification of U and Pu. Salt-free reagents are used in the solvent washing process as well as the SEIFICS process as a salting-out reagent. For the mass balance, in the reprocessing plant with the capacity of 200tHM/y using the NEXT process for example, 1t of U, Pu, Np, Am and Cm are reprocessed: Pu/(U+Pu) ratio is 0.1 in the dissolver solution, 0.3 in the feed solution of the extraction process after the crystallization .

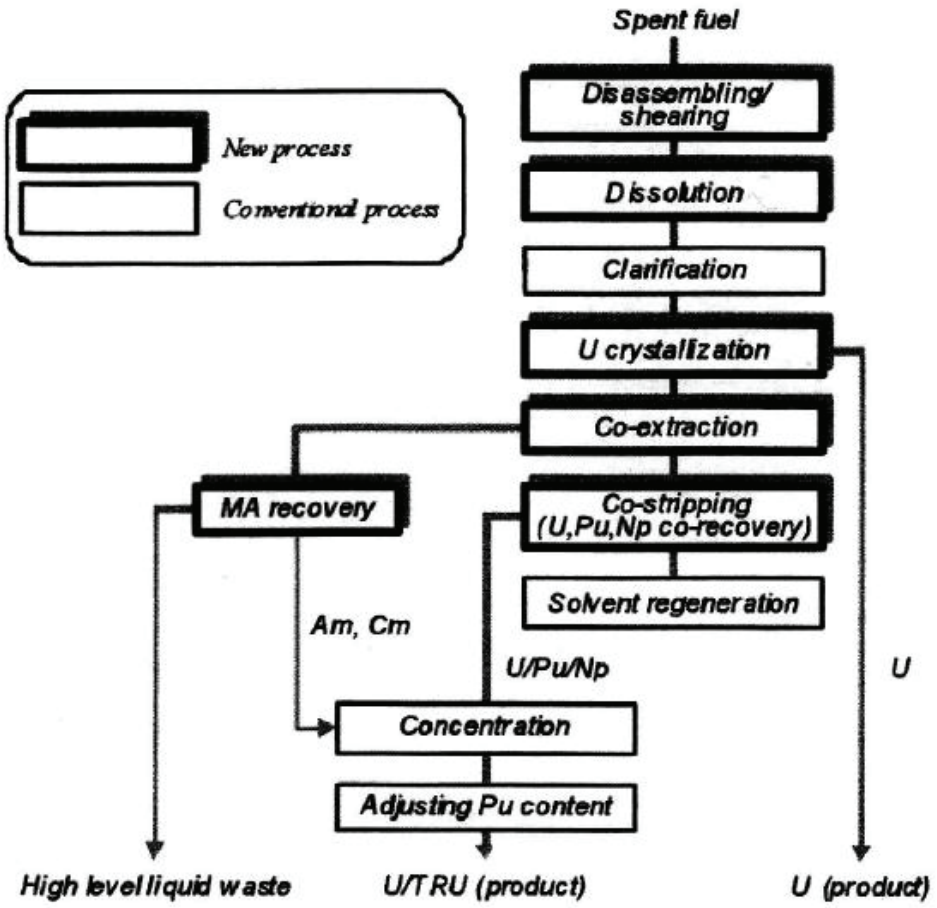

Figure 1.1 Schematic flow of the NEXT process

References

1. Pearce; Joshua open access; "Photovoltaics – A Path to Sustainable Futures"; Futures 34 (7) 663–674 (2002)

2. Vick, B.D., Clark, R. N.; ‘‘Effect of panel temperature on a Solar-PV AC water pumping system’’, Proceedings of the International Solar Energy Society (ISES), 159–164 (2005)

3. Fthenakis, V.; Kim, H. C. "Land use and electricity generation: A life-cycle analysis". Renewable and Sustainable Energy Reviews, 13 (6–7) 1465 (2009)

4. Kakati B. K., Mohan V., "Development of low cost advanced composite bipolar plate for P.E.M. fuel cell", Fuel Cells, 08(1) 45–51 (2008)

5. Kakati, B. K., Deka, D., "Effect of resin matrix precursor on the properties of graphite composite bipolar plate for PEM fuel cell", Energy & Fuels, 21 (3)1681–1687 (2007)

6. S. Giddey, S.P.S. Badwal, A. Kulkarni, C. Munnings; "A comprehensive review of direct carbon fuel cell technology"; Progress in Energy and Combustion Science; 38 (3): 360–399 (2012)

7. G. Brumfiel; "Chaos could keep fusion under control"; Nature, (2006).

8. R.W. Bussard; "Should Google Go Nuclear? Clean, Cheap, Nuclear Power"; Google TechTalks; (2006)

9. P. Gary Eller, Bob Penneman, and Bob Ryan; "Pioneer actinide chemist Larned Asprey dies"; The Actinide Research Quarterly, Los Alamos National Laboratory, pp. 13–17.(1st quarter 2005)

10. J.H. Burns; "Solvent-extraction complexes of the uranyl ion; Crystal and molecular structures of catena-bis(.mu.-di-n-butyl phosphato-O,O')dioxouranium(VI) and bis(.mu.-di-n-butyl phosphato-O,O')bis[(nitrato)(tri-n-butylphosphine oxide)dioxouranium(VI)]". Inorganic Chemistry 22 (8) 1174 (1983).

11. Greenwood, Norman N.; Earnshaw, Alan. Chemistry of the Elements Butterworth-Heinemann. p.1261 (1997)

12. G.H. John, I. May, M.J. Sarsfield, H.M. Steele, D. Collison, M. Helliwell and J.D. McKinney; "The structural and spectroscopic characterisation of three actinyl complexes with coordinated and uncoordinated perrhenate"; Dalton Trans (5) 734 (2004)

13. Gerber, M.S.; "History of Hanford Site Defense Production (Brief)"; Fluor Hanford / US DOE (2001)

14. Martin, Hugo; "Nuclear site now a tourist hot spot"; The Los Angeles Times; (2008)

15. Nakahara, S.; “U, Pu and Np Co-recovery in simplified Solvent Extraction Process”; JAEA-Research 2006-030, 43p (2006)

Chapter2

Properties of reaction crystallization

2.1 Nucleation phenomenon [11]

Nucleation phenomenon is indicates that new phase occurs from the homogeneous gas phase and the liquid phase. In this new phase, gas, liquid and solid phase coexist, but for them, there is a common treatment. The phenomenon of nucleation in the crystallization, new solid phase is produced from the liquid phase. Here，nucleation phenomena of crystallization can be classified into several kinds (Figure .2.1).

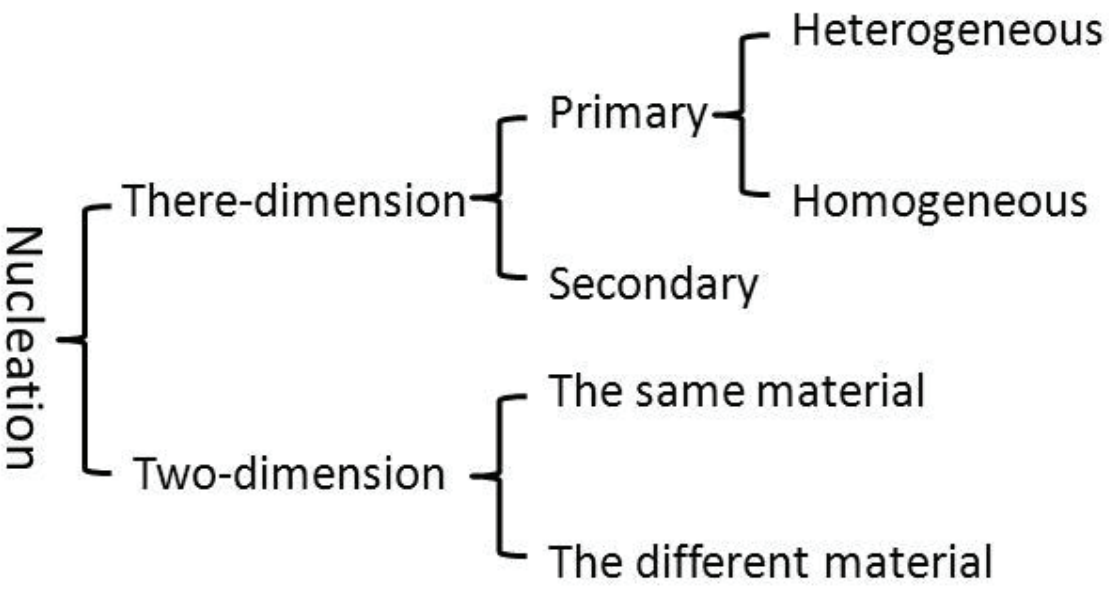

Figure .2.1 Nucleation

2.2 Primary nucleation phenomenon

Primary nucleation phenomenon occurs when crystal nuclei spontaneously appear in supersaturated solution in the absence of same crystals. It is to be the root of the crystalline product. Homogeneous nucleation phenomenon happens in single substance liquid phase solution, and super saturation state takes place in this occasion. Heterogeneous nucleation phenomenon (Heterogeneous Nucleation) the phenomenon of solid phase, such as the dissolved impurities from the wall of the apparatus and other impurities are present, nucleation occurs is due to the contribution of these. On an industrial device, uniform nucleation phenomenon is very small.

In over-saturated solution, the compound solute is generated by the collision of the solute. This grows disappears in the solution. However, the magnitude of growth exists even though actually growth has disappeared. Defining that crystal nuclear is critical grain size, this size is referred to as a "germ".

2.3 Crystallizer design

Uranium crystallization based on solubility difference is one of the remarkable technologies which can provide simple reprocessing process to separate uranium in nitric acid solution since the process is mainly controlled by temperature and concentration of solute ions. Japan Atomic Energy Agency (JAEA) and Mitsubishi Materials Cooperation MMC) are developing the crystallization process for crystallization technology of FBR fuel reprocessing. [l-3] The uranium(U) crystallization process is a key technology for New Extraction System for TRU Recovery (NEX1) process that was evaluated as the most promising process for future FBR reprocessing .[4-6] We had developed an innovative crystallizer and carried out several fundamental investigation. On the basis of the results, we fabricated an engineering scale crystallizer and have carried out continuous crystallization test to investigate the stability of the equipment at steady and non-steady state conditions by using developed uranium. As for simulating typical failure events in the crystallizer, crystal accumulation and crystal blockage were induced and monitoring method and resuming procedure were evaluated in this work, no significant phenotletloll was observed in the steady state test and all failure events are proven to be recovered by appropriate resumed procedures. Outline of the annular type continuous crystallizer is shown in Figure 2.2 and Figure 2.3. This crystallizer is designed for continuous operation adopting high throw put and equipment scale-up. A rotary driven cylinder has a screw blade to transfer UNH crystals sulrry, and annular a shaped space is formed as crystallization section in between the rotary cylinder and outer cylinder.

This device is considered about criticality safety with geometrical control and maintainability for remote operation. Dissolver solution is fed into the annular section from the feed line at the bottom end of the outer cylinder, and coolant is fed into cooling jacket on the cylinder. The solute the liquid is drained out from a nozzle at middle part of the clynder. The discharged uranyl nitrate crystals slurry is still accompanied with a little solution. Therefore it needs to be dried by the crystals separate or as centrifugal dewatering process.

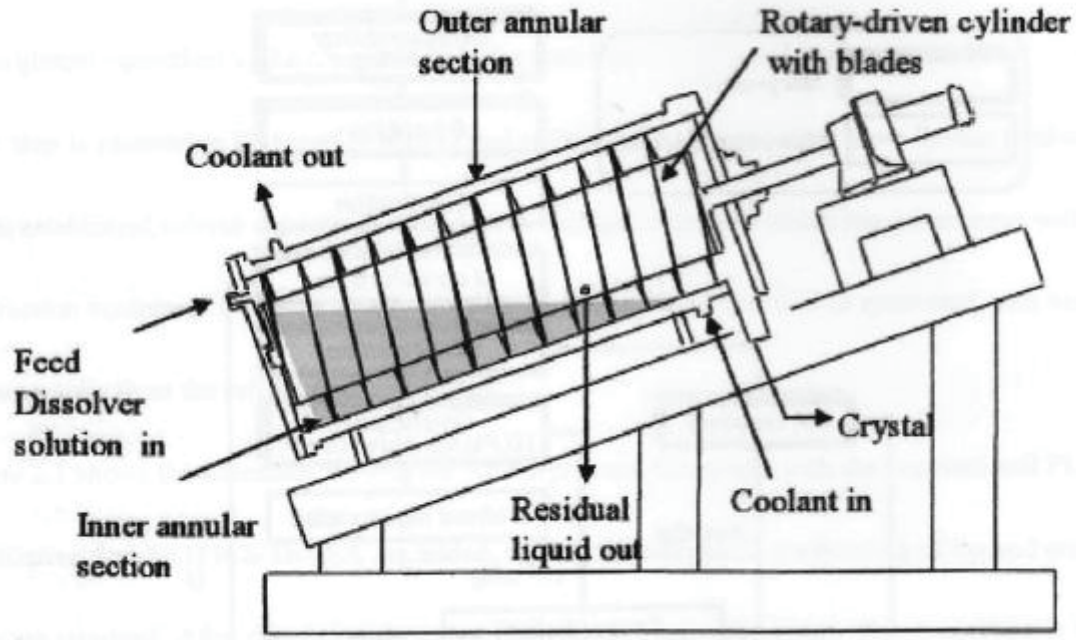

Figure 2.2 0utline of the annular type continuous crystallizer

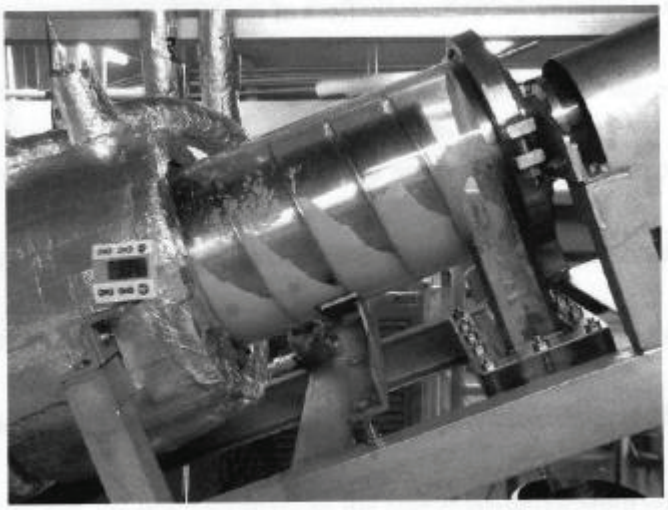

Figure 2.3 Running crystallizer

2.4 Melt Crystallization of uranium

The crystallization is considered one of the key technologies for uranium recovery from the spent fuel in the future reprocessing plant (Figure 2.4), because it promises much desired safety and economical efficiency. The crystallization is a separation technology based on differences in solubility, executed by changing temperature and concentration, with no organic reagent needed, so that the separation system can be simple.

Since 1990s, JAEA has been carrying out small scale hot experiments at the Chemical Processing Facility (CPF), and development of an engineering-scale system is being carried out. In the hot experiments, the uranium recovery rate, the decontamination factors of plutonium, and fission products (FPs) have been confirmed, and the crystal purification technology have been investigated.

In research for practical application, we selected a rotary driven type crystallizer which has the advantages of criticality safety, high throughput, and remote maintenance, etc.

The uranium crystal is generated in the cooled solution in the crystallizer, and the crystal is isolated from residual solution (mother solution) by the cylinder rotation and is discharged from the device. In the system development of the engineering scale system, we fabricated an engineering scale crystallizer system, and have been investigating the properties of steady and non-steady state operations. In these investigations, the operation conditions for stable crystallization, the crystal accumulation and blockage phenomena during crystal discharge, and the outlet of mother solution are being confirmed. The crystal accumulation can be monitored by a cylinder torque meter, and the event can be overcome by the stoppage of feed solution and stepwise increment of the screw speed. Development of the instrumentation and control system also is progressing.

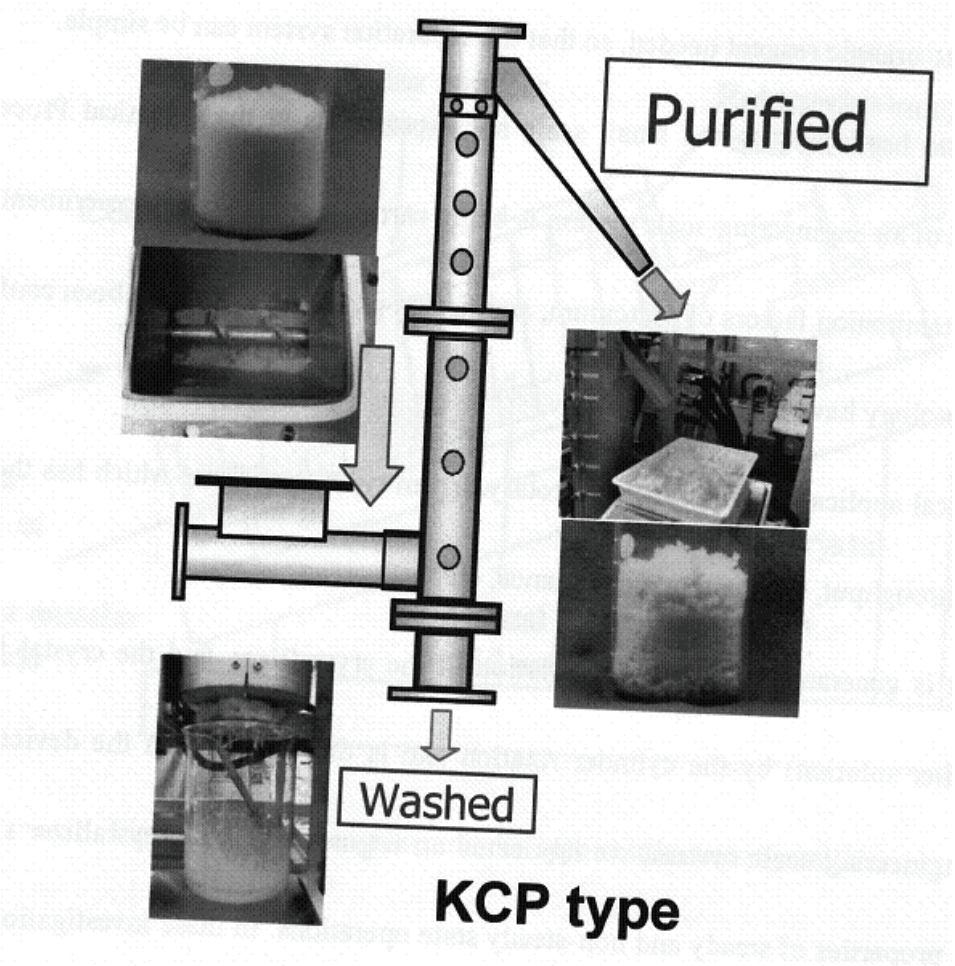

Figure 2.4 Running melt crystallizer

References

1. Chikazawa, T., T. Kikuchi, A. Shibata, T. Koyama and S. Homma; "Batch Crystallization of Uranyl Nitrate," J Nucl . Sci. Technol., 45, 6, 582-587 (2008)

2. Henrich, E., H. Schmieder and K. Ebert; "Combination of IBP Extraction and Nitrate Crystallization for Spent Nuclear Fuel Reprocessing," Inst. Chem. Eng. Symp. Ser., 103, 191-205 (1987)

3. Homma, S., J. Ishii, T. Kikuchi, T. Chikazawa, A. Shibata, T. Koyama, J. Koga and S. Matsumoto; "Flowsheet Study of U-Pu Co-Crystallization Reprocessing System," J Nucl. Sci. Technol., 45, 510-517 (2008)

4. Matsuoka, M., S. Kasama and M. Ohishi; "Purification of p-Dichlorobenzen and m-Chloronitromenzene Crystalline Particles," J Chem. Eng. Japan., 19,181(1986)

5. Matsuoka, M., T. Fukuda, Y. Takagi and H. Takiyama; "Purification by Sweating of Organic Solid Solurions by Layer and Suspension Type Melt Crystallization Operations," J Chem. Eng. Japan., 28, 562-569 (1995)

6. Otawara, K. and K. Matsuoka; "Axial Dispersion in a Kureha Crystal Purifier (KCP)," J Cryst. Growth, 237-239, 2246-2250 (2002)

7. Shibata, A., K. Ohyama, K. Yano, K. Nomura, T. Koyama, K. Nakamura, T. Kikuchi and S. Homma; "Experimental Study on U-Pu Cocrystallization Reprocessing Process," J Nucl. Sci. Technol., 46, 204-209 (2009)

8. Takata, T., Y. Koma, K. Sato, M. Kamiya, A. Shibata, K. Nomura, H. Ogino, T. Koyama and S. Aose; "Conceptual Design Study on Advanced Aqueous Reprocessing System for Fast Reactor Fuel Cycle," J Nucl . Sci. Technol., 41, 307-314 (2004)

9. Ulrich, J. and H. Glade; -Melt-Crystallization Fundamentals, Equipment and Applications, Shaker Verlag, Aachen, Germany (2003)

10. Yano, K., A. Shibata, K. Nomura, T.Koizumi, T. Koyama and C. Miyake; "Plutonium Behavior under the Condition of Uranium Crystalliz.ation from Dissolver Solution," Proc. Int. Conf ATALANTE2004, pp. 1-66, Nimes, France (2004)

11. J. W. Mullin, ‘‘Crystallization 44th ed. Butterworth-Heinemann, Oxford, 2001.

Chapter3

Adsorption-desorption mechanism and ZMH encrustation preventing methods

3.1 Adsorption

Adsorption is the adhesion of atoms, ions, or molecules from a gas, liquid, or dissolved solid to a surface. This process creates a film of the adsorbate on the surface of the adsorbent. This process differs from absorption, in which a fluid (the absorbate) permeates or is dissolved by a liquid or solid (the absorbent). Note that adsorption is a surface-based process while absorption involves the whole volume of the material. The term sorption encompasses both processes, while desorption is the reverse of adsorption. It is a surface phenomenon results, particularly when the interaction energy is low.

Similar to surface tension, adsorption is a consequence of surface energy. In a bulk material, all the bonding requirements (be they ionic, covalent, or metallic) of the constituent atoms of the material are filled by other atoms in the material. However, atoms on the surface of the adsorbent are not wholly surrounded by other adsorbent atoms and therefore can attract adsorbates. The exact nature of the bonding depends on the details of the species involved, but the adsorption process is generally classified as physisorption (characteristic of weak van der Waals forces) or chemisorption (characteristic of covalent bonding). It may also occur due to electrostatic attraction. [1]

Adsorption is present in many natural physical, biological, and chemical systems, and is widely used in industrial applications such as activated charcoal, capturing and using waste heat to provide cold water for air conditioning and other process requirements (adsorption chillers), synthetic resins, increase storage capacity of carbide-derived carbons, and water purification. Adsorption, ion exchange, and chromatography are sorption processes in which certain adsorbates are selectively transferred from the fluid phase to the surface of insoluble, rigid particles suspended in a vessel or packed in a column. Lesser known, are the pharmaceutical industry applications as a means to prolong neurological exposure to specific drugs or parts thereof.

3.2 Electonic states of solid surface

Surface chemistry can be roughly defined as the study of chemical reactions at interfaces. It is closely related to surface engineering, which aims at modifying the chemical composition of a surface by incorporation of selected elements or functional groups that produce various desired effects or improvements in the properties of the surface or interface. Surface chemistry also overlaps with electrochemistry. Surface science is of particular importance to the field of heterogeneous catalysis.

The adhesion of gas or liquid molecules to the surface is known as adsorption. This can be due to either chemisorption or by physisorption. These too are included in surface chemistry.

The behavior of a solution based interface is affected by the surface charge, dipoles, energies, and their distribution within the electrical double layer.

Surface physics can be roughly defined as the study of physical changes that occur at interfaces. It overlaps with surface chemistry. Some of the things investigated by surface physics include surface states, surface diffusion, surface reconstruction, surface phonons and plasmons, epitaxy and surface enhanced Raman scattering, the emission and tunneling of electrons, spintronics, and the self-assembly of nanostructures on surface.

The study and analysis of surfaces involves both physical and chemical analysis techniques.

Several modern methods probe the topmost 1–10 nm of surfaces exposed to vacuum. These include X-ray photoelectron spectroscopy, Auger electron spectroscopy, low-energy electron diffraction, electron energy loss spectroscopy, thermal desorption spectroscopy, ion scattering spectroscopy, secondary ion mass spectrometry, Dual polarization interferometry, and other surface analysis methods included in the list of materials analysis methods. Many of these techniques require vacuum as they rely on the detection of electrons or ions emitted from the surface under study. Moreover, in general ultra high vacuum, in the range of 10−7 pascal pressure or better, is necessary to reduce surface contamination by residual gas, by reducing the number of molecules reaching the sample over a given time period. At 0.1 mPa (10−6 Torr), it only takes 1 second to cover a surface with a contaminant, so much lower pressures are needed for measurements.

Purely optical techniques can be used to study interfaces under a wide variety of conditions. Reflection-absorption infrared, dual polarisation interferometry, surface enhanced Raman, and sum frequency generation spectroscopies can be used to probe solid–vacuum as well as solid–gas, solid–liquid, and liquid–gas surfaces. Dual Polarization Interferometry is used to quantify the order and disruption in birefringent thin films. [2] This has been used, for example, to study the formation of lipid bilayers and their interaction with membrane proteins.

Modern physical analysis methods include scanning-tunneling microscopy (STM) and a family of methods descended from it. These microscopies have considerably increased the ability and desire of surface scientists to measure the physical structure of many surfaces. This increase is related to a more general interest in

nanotechnology.

3.3 Isoelectric point [3]

The isoelectric point (pI), sometimes abbreviated to IEP, is the pH at which a particular molecule or surface carries no net electrical charge.

Amphoteric molecules called zwitterions contain both positive and negative charges depending on the functional groups present in the molecule. The net charge on the molecule is affected by pH of its surrounding environment and can become more positively or negatively charged due to the gain or loss, respectively, of protons (H+). The pI is the pH value at which the molecule carries no electrical charge or the negative and positive charges are equal.

Surfaces naturally charge to form a double layer. In the common case when the surface charge-determining ions are H+/OH-, the net surface charge is affected by the pH of the liquid in which the solid is submerged.

The pI value can affect the solubility of a molecule at a given pH. Such molecules have minimum solubility in water or salt solutions at the pH that corresponds to their pI and often precipitate out of solution. Biological amphoteric molecules such as proteins contain both acidic and basic functional groups. Amino acids that make up proteins may be positive, negative, neutral, or polar in nature, and together give a protein its overall charge. At a pH below their pI, proteins carry a net positive charge; above their pI they carry a net negative charge. Proteins can, thus, be separated according to their isoelectric point (overall charge) on a polyacrylamide gel using a technique called isoelectric focusing, which uses a pH gradient to separate proteins. Isoelectric focusing is also the first step in 2-D gel polyacrylamide gel electrophoresis.

3.4 Covalent bond

A covalent bond is a chemical bond that involves the sharing of electron pairs between atoms. The stable balance of attractive and repulsive forces between atoms when they share electrons is known as covalent bonding. [4] For many molecules, the sharing of electrons allows each atom to attain the equivalent of a full outer shell, corresponding to a stable electronic configuration.

Covalent bonding includes many kinds of interactions, including σ-bonding, π-bonding, metal-to-metal bonding, agostic interactions, and three-center two-electron bonds.[5][6] The term covalent bond dates from 1939. The prefix co- means jointly, associated in action, partnered to a lesser degree, etc.; thus a "co-valent bond", in

essence, means that the atoms share "valence", such as is discussed in valence bond theory. In the molecule H 2, the hydrogen atoms share the two electrons via covalent bonding. Covalency is greatest between atoms of similar electronegativities. Thus, covalent bonding does not necessarily require that the two atoms be of the same elements, only that they be of comparable electronegativity. Covalent bonding that entails sharing of electrons over more than two atoms is said to be delocalized.

3.5 Electrostatic attraciton

In the surface of the solid and aqueous solution where charged to the positive or negative. Metal oxide and natural polymers are charged to the negative on where isoelectric point on the alkaline side while charged to positive on the acidic side. Also, in ionic crystals each lattice point is positive and negative regularly lined. The adsorption quality understandably ions, the ions and charged points of interface between acting electrostatic attraction. Also, when approached with higher dielectric constant of solid Ionic solid surface opposite charge, Ion is attracted to the surface. For example, when occurs at the interface of metal oxides and water and negatively charged hydrogen ions and dissociated ions, metal ions, both detained in electrostatic attraction, could not completely leave the distribution near the interface between the Interfacial double layer forming. Hydrogen ions will can move into the aqueous solution from the electric double layer, adsorption of cationic ion by adsorption and electrostatic attraction of positively charged surface, underwater and there other cations. The Exchange adsorption is called ion exchange. As this example is a representative variety of cations in water by cation exchange resin adsorption. Solid-charged molecule with a bipolar child as well as ions in charged liquid surface or Interfacial vivo-induced dipole electrostatic attraction, adsorbed molecules causing too weak. [3]

3.6 Hydrogen bond

A hydrogen bond is the electromagnetic attractive interaction between polar molecules in which hydrogen (H) is bound to a highly electronegative atom, such as nitrogen (N), oxygen (O) or fluorine (F). The name hydrogen bond is something of a misnomer, as it is not a true bond but a particularly strong dipole-dipole attraction, and should not be confused with a covalent bond.

These hydrogen-bond attractions can occur between molecules (intermolecular) or within different parts of a single molecule (intramolecular). The hydrogen bond (5 to 30 kJ/mole) is stronger than a van der Waals interaction, but weaker than covalent or ionic bonds. This type of bond can occur in inorganic molecules such as

water and in organic molecules like DNA and proteins.

Intermolecular hydrogen bonding is responsible for the high boiling point of water (100 °C) compared to the other group 16 hydrides that have no hydrogen bonds. Intramolecular hydrogen bonding is partly responsible for the secondary and tertiary structures of proteins and nucleic acids. It also plays an important role in the structure of polymers, both synthetic and natural.

In 2011 an IUPAC Task Group recommended a modern evidence-based definition of hydrogen bonding. The new definition was published in the IUPAC journal Pure and Applied Chemistry. [7] This detailed technical report provides the rationale behind the new definition. [8]

3.7 Van der Waals force

For macroscopic bodies with known volumes and numbers of atoms or molecules per unit volume, the total van der Waals force is often computed based on the "microscopic theory" as the sum over all interacting pairs. It is necessary to integrate over the total volume of the object, which makes the calculation dependent on the objects' shapes. For example, the van der Waals' interaction energy between spherical bodies of radii R1 and R2 and with smooth surfaces was approximated in 1937 by Hamaker. [9]

The van der Waals forces between objects with other geometries using the Hamaker model have been published in the literature. [11][12][13]

From the expression above, it is seen that the van der Waals force decreases with decreasing particle size (R). Nevertheless, the strength of inertial forces, such as gravity and drag/lift, decrease to a greater extent. Consequently, the van der Waals forces become dominant for collections of very small particles such as very fine-grained dry powders (where there are no capillary forces present) even though the force of attraction is smaller in magnitude than it is for larger particles of the same substance. Such powders are said to be cohesive, meaning they are not as easily fluidized or pneumatically conveyed as easily as their more coarse-grained counterparts. Generally, free-flow occurs with particles greater than about 250 μm.

The van der Waals' force of adhesion is also dependent on the surface topography. If there are surface asperities, or protuberances, that result in a greater total area of contact between two particles or between a particle and a wall, this increases the van der Waals force of attraction as well as the tendency for mechanical interlocking.

The microscopic theory assumes pairwise additivity. It neglects many-body interactions and retardation. A more

rigorous approach accounting for these effects, called the "macroscopic theory," was developed by Lifshitz in 1956. [14] Langbein derived a much more cumbersome "exact" expression in 1970 for spherical bodies within the framework of the Lifshitz theory [15] while a simpler macroscopic model approximation had been made by Derjaguin as early as 1934. [16] Expressions for the van der Waals forces for many different geometries using the Lifshitz theory have likewise been published.

3.8 Hydrophobic effect

The hydrophobic effect is the observed tendency of nonpolar substances to aggregate in aqueous solution and exclude water molecules. The name, literally meaning "water-fearing," describes the segregation and apparent repulsion between water and nonpolar substances. The hydrophobic effect explains the separation of a mixture of oil and water into its two components, and the beading of water on nonpolar surfaces such as waxy leaves. At the molecular level, the hydrophobic effect is important in driving protein folding, [17][18] formation of lipid bilayers and micelles, insertion of membrane proteins into the nonpolar lipid environment and protein-small molecule interactions. Substances for which this effect is observed are known as hydrophobes.

Reference

1. Ferrari, L., Kaufmann, J., Winnefeld, F., Plank, J.; "Interaction of cement model systems with super plasticizers investigated by atomic force microscopy, zeta potential, and adsorption measurements". J Colloid Interface Sci. 347 (1)15–24. (2010)

2. Mashaghi, A, Swann, M, Popplewell, J, Textor, M, Reimhult, E.; "Optical Anisotropy of Supported Lipid Structures Probed by Waveguide Spectroscopy and Its Application to Study of Supported Lipid Bilayer Formation Kinetics". Analytical Chemistry 80 (10) 3666 (2008)

3. Takeuti, S.; ‘‘Kyuthakunokagaku’’, Sangyotosho, 39(1995)

4. Campbell, Neil A., Brad Williamson, Robin J. Heyden.; ‘‘Biology: Exploring Life’’; Boston, Massachusetts, Pearson Prentice Hall (2006)

5. March, Jerry; ‘‘Advanced organic chemistry: reactions, mechanisms, and structure’’; John Wiley & Sons (1992)

6. Gary L. Miessler. Donald Arthur Tarr.; ‘‘Inorganic chemistry’’, Prentice Hall (2004)

7. E. Arunan, G. R. Desiraju, R. A Klein, J. Sadlej, S. Scheiner, I. Alkorta, D. C. Clary, R. H. Crabtree, J. J. Dannenberg, P. Hobza, H. G. Kjaergaard, A. C. Legon, B. Mennucci, and D. J. Nesbitt. "Definition of the hydrogen bond"; Pure Appl. Chem. 83 (8) 1637–1641 (2011)

8. E. Arunan, G. R. Desiraju, R. A Klein, J. Sadlej, S. Scheiner, I. Alkorta, D. C. Clary, R. H. Crabtree, J. J. Dannenberg, P. Hobza, H. G. Kjaergaard, A. C. Legon, B. Mennucci, and D. J. Nesbitt. "Defining the hydrogen bond: An Account"; Pure Appl. Chem. 83 (8) 1619–1636 (2011)

9. H. C. Hamaker, Physica, 4(10), 1058-1072 (1937)

10. F. London, Transactions of the Faraday Society, 33, 8-26 (1937)

11. R. Tadmor, JOURNAL OF PHYSICS: CONDENSED MATTER, 13 (2001) L195–L202

12. Israelachvili J., Intermolecular and Surface Forces, Academic Press (1985–2004),

13. V. A. Parsegian, "Van der Waals Forces: A Handbook for Biologists, Chemists, Engineers, and Physicists," Cambridge University Press (2006)

14. E. M. Lifshitz, Soviet Phys. JETP, 2, 73 (1956)

15. D. Langbein, Phys. Rev. B, 2, 3371 (1970)

16. B. V. Derjaguin, Kolloid-Z., 69, 155-64 (1934)

17. Kauzmann W.; "Some factors in the interpretation of protein denaturation"; Advances in Protein Chemistry 14 1–63. (1959)

18. Charton, M., Charton, B. I.; "The structural dependence of amino acid hydrophobicity parameters". Journal of Theoretical Biology 99 (4) 629–644(1982)

Chapter4

ZMH crystal growth on reaction crystallization

4.1 **Introduction**

In the nuclear electric power generation, a variety of impurities, called as “fission products”, are produced by uranium fuel nuclear fission reaction [1]. In the dissolution step of spent nuclear fuels, there is a world-concern problem that zirconium molybdate hydrate (ZMH) precipitates as a byproduct, which accumulates in the reprocessing equipments [2–4]. In order to remove the accumulation, various physical and chemical cleaning methods have been reported. But, these methods have induced new problems. For examples, workers who enter into the device are at risk of being exposed to radiation if removing the accumulation with high pressure water; equipments and pipes would be corroded if using acid or alkaline [6–8]. More recently, Japan Atomic Energy Agency has reported that less accumulation was observed in the reprocessing equipments when small round zirconium metals were added. The reason is that the major component of accumulation ZMH is easier to stick on the surface of the zirconium metal rather than that of the equipment. However, this method is expensive and difficult in reuse [9]. In this paper, we report a new method based on crystallization engineering to prevent the accumulation. This method is based on the control of crystallized reaction of the ZMH in the waste solution, followed by a solid-liquid separation. The particle size of the ZMH was studied by batch crystallization experiments with different nitrate concentration and operating temperature.

4.2Experimental methods

In nitric acid, the ZMH is produced by the reaction of sodium molybdenum (VI) dihydrate and zirconyl nitrate dehydrate. The mechanism of this reaction is shown as follow Eq. 1.

$$2HMoO_4^- + ZrO_2^+ + 2H_2O \rightarrow Zr(OH)_2Mo_2O_7(H_2O)_2 \quad (2.1)$$

4.2.1 Materials

Molybdenum (VI) in nitric acid (from 61.3% nitric acid, Wako, Japan) was prepared by dissolving sodium molybdate dihydrate (Na2MoO4·2H2O, Wako, Japan). Zirconium (IV) in nitric acid awas prepared by dissolving reagent grade zirconyl nitrate dehydrate (ZrO(NO3)2·2H2O, Wako, Japan). By mixing this molybdenum and zirconium solutions, the concentration of molybdenum was controlled as the level of 0.1 M, and the concentration of zirconium was controlled as the level of 0.05 M. And the concentration of nitric acid of this mixing solution was controlled at the level of 3M or 5 M.

4.2.2 Crystal size measurements.

First, pour the above mixing solution (100 mL) into a beaker. Second, operating temperatures were varied from 343 K to 373 K as shown in Table 1. At each concentration of nitric acid and operating temperatures, the ZMH crystallized and samples were prepared, as shown in Fig. 1. After ZMH crystal samples were dehydrated for one day, they were observed by X-ray diffraction (XRD) and also by scanning electronmicroscopy (SEM).

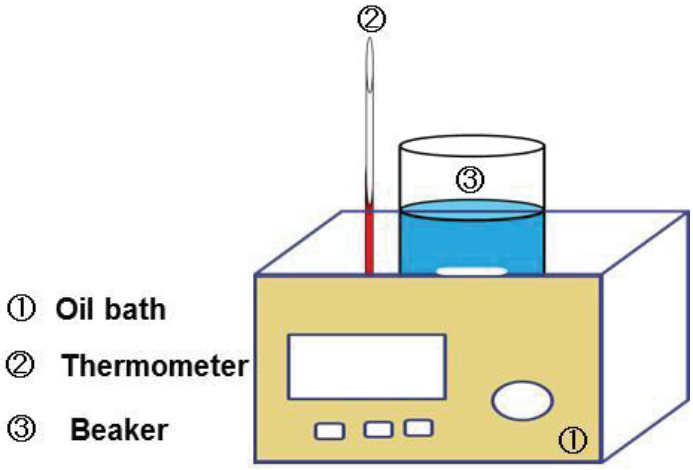

Fig. 4.1 Experimental apparatus

Tab. 4.1 Experimental condition

Concentration of $ZrO(NO_3)_2 \cdot 2H_2O$	[mol/L]	0.05
Concentration of $Na_2MoO_4 \cdot 2H_2O$	[mol/L]	0.1
Concentration of HNO_3	[mol/L]	3, 5
Reaction time	[hr]	2
Reaction temperature	[K]	343-373

4.2.3 Polymorph of ZMH crystal

At first, pour the mixing solution (from 2.1, 100 mL) into a reactor. And then, operating temperatures were setup as shown in Table 2. At the concentration of 3M nitric acid, the ZMH was crystallized for 24 h by using an experimental apparatus shown in Fig. 1. In addition, samples were taken after one hour. At the concentration of 1M nitric acid, after the ZMH was crystallized for 2 h, ZMH crystals were dehydrated for a day. Then the ZMH crystals were analyzed by XRD and SEM.

Tab. 4.2 Experimental condition

Concentration of $ZrO(NO_3)_2 \cdot 2H_2O$	[mol/L]	0.05
Concentration of $Na_2MoO_4 \cdot 2H_2O$	[mol/L]	0.1
Concentration of HNO_3	[mol/L]	1, 3
Reaction time	[hr]	24
Reaction temperature	[K]	343-363

4.2.4Preventing ZMH accumulation with single jet method

Experimental condition is shown as Table 1. In this section, batch method and single jet method were both conducted. First, the mix solution (from 2.1) 180ml was prepared in a test tube. The ZMH was crystallized at 90 degree Celsius for 2 hours using a batch method. The samples of concentration of solution were collected at 0, 10, 20, 30, 60, 120, 180, 240 minutes after starting the reaction. Next, 60 ml of $ZrO(NO_3)_2$ solution (from 2.1) was heated at 90 degree Celsius in a test tube. After that, 120 ml of Na_2MoO_4 solution was added at a speed of 1 ml/min for 2 hours, and at a speed of 0.3 ml/min in 6 hours with single jet method, Figure 1. The samples of concentration of solution were made at 2 and 6 hours after starting to add Na_2MoO_4 solution into the test tube. ZMH crystal samples were observed by Scanning Electron Microscopy (SEM). The samples of concentration of solution were measured by Inductively Coupled Plasma- Mass Spectrometry (ICP-MS).

4.3 Results and discussion

4.3.1 Basic data of ZMH

4.3.1.1 Behavior of ZMH crystals

After the reaction, there were white and yellow stickings on the inner surface of the beaker as showing in Fig. 2. Fig. 3 shows that the XRD pattern of the mixture of white and yellow stickings, which agreed to that of

ZrMo2O7(OH)2.

Fig. 4.2 Produced ZMH crystal

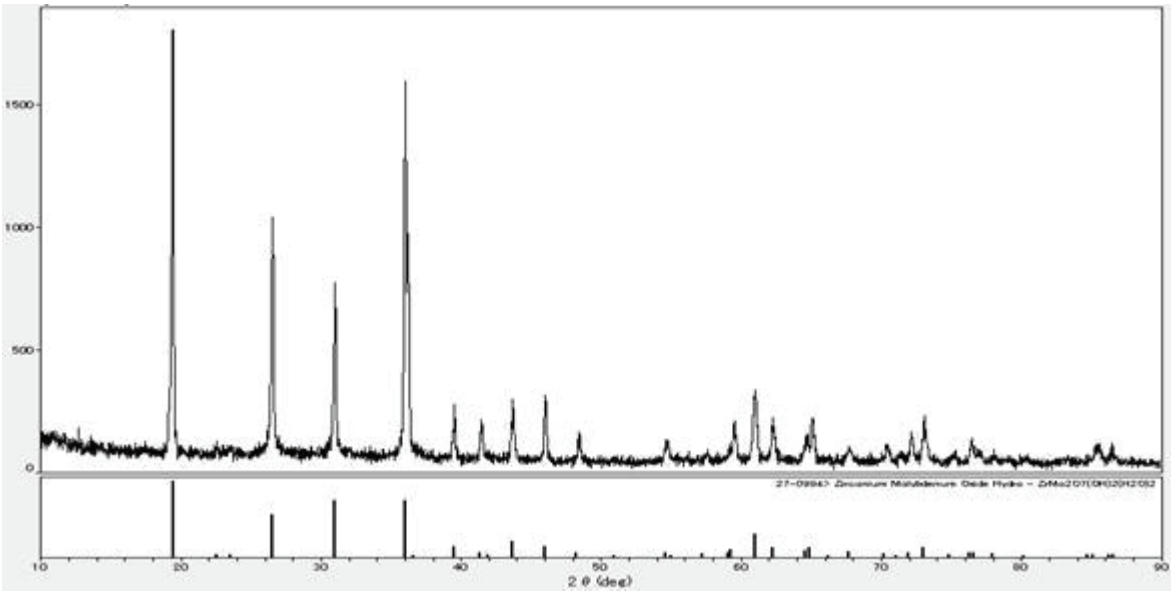

Fig. 4.3 XRD of ZMH

4.3.1.2 White precipitation observing

Fig. 5 shows the SEM images of white sticking. Two different surfaces of the white sticking can be observed: one with a tightly bonded structure appeared on the inner surface of the beaker; on another one, ZMH crystal grew up in an inhomogeneous manner. Therefore, it can be considered that the small particles would stick on the inner surface of the beaker when ZMH began to nucleate; after white sticking was produced completely, ZMH crystal would grow up on the surface of white sticking. As the particle grows up, the crystal becomes yellow.

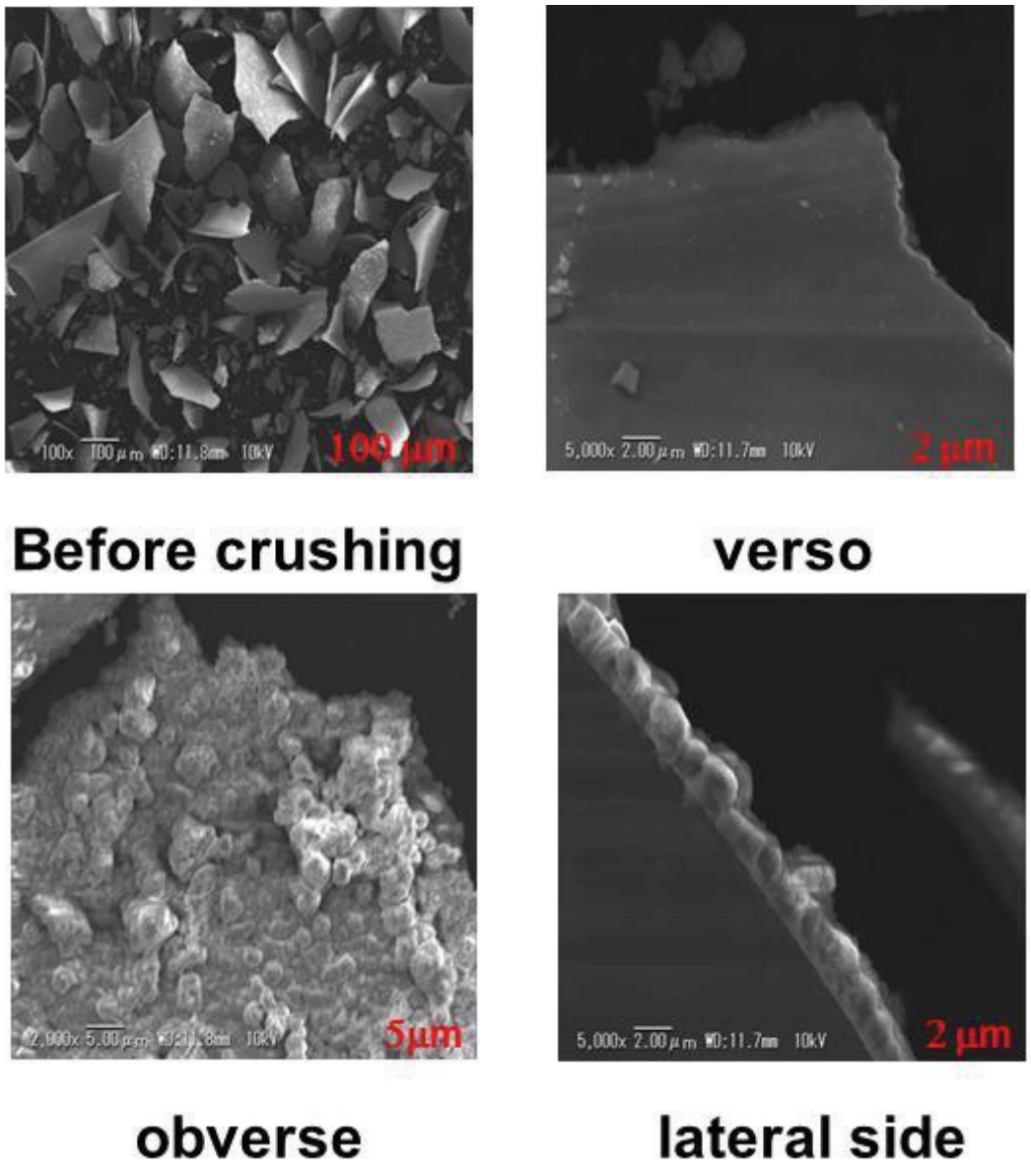

Fig. 4.4 Observed white sticking

4.3.1.3 Solubility of ZMH in nitric acid

Figure 7 shows the solubility of ZMH in nitric acid (at the levels of 3M and 5 M). At each concentration of nitric acid, the solubility of ZMH decreases with increasing operating temperature. At 343 K, the solubility of ZMH is higher in 5M nitric acid than in 3M nitric acid. On the contrary, when the temperature is over 353 K, the solubility of ZMH is lower in 5M nitric acid than 3M nitric acid. At the same time, the solubility of Mo decreases suddenly, because Mo might crystallize as different crystal at high level of nitric acid concentration.

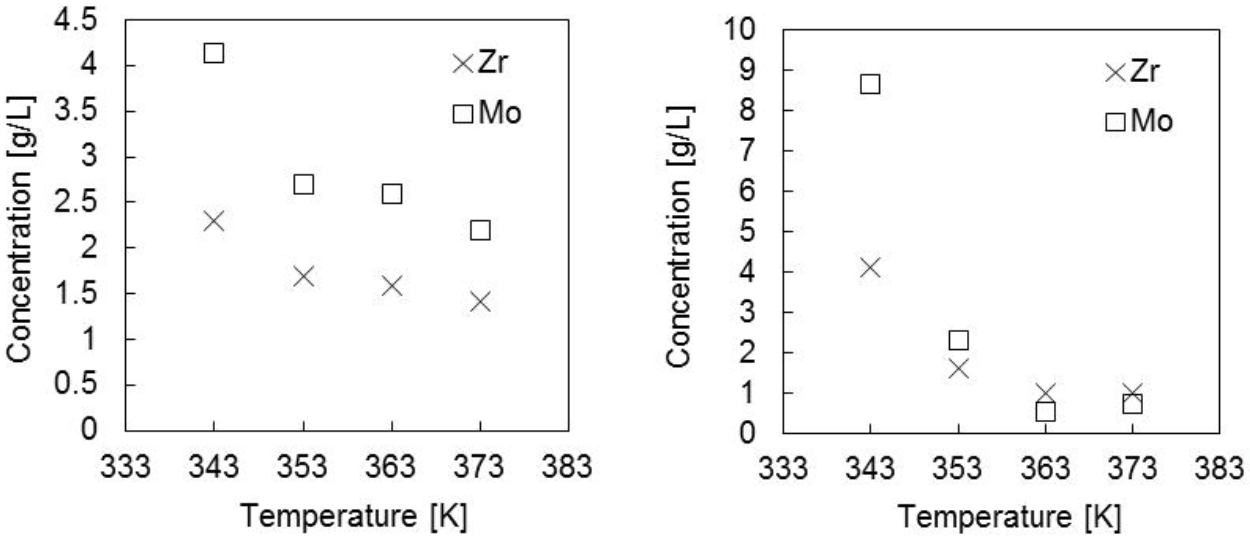

3N nitric acid **5N nitric acid**

Fig. 4.5 solubility of ZMH in nitric acid

4.3.2 Polymorph of ZMH

This experiment was performed using 1N HNO3. White precipitates were observed while Mo solution was added into Zr solution (the level of concentration of Mo and Zr is the same level as the Experiment 2.2). The experiment shows that supersaturation of ZMH in 1M HNO3 is higher than that in 3M or 5M HNO3. Therefore we can suppose that the lower the concentration of HNO3, the lower the solubility of ZMH. Then only white precipitates were observed after heating at 353 K for 2 h. Therefore, the white precipitates showed strong

adhesiveness, and got to one lump after ZMH were dried for one night. Fig. 8 shows the SEM image of ZMH crystal sample which was precipitated in 1M HNO3. Agglomerated and pillared crystals were observed with the average long particle size of 0.5 μm. Fig. 9 shows the XRD pattern of the crystal precipitated in 1MHNO3, which agreed with that of ZMH. Comparing with Fig. 3, it is easy to find that there are several different peaks in the range of 20°<2θ<40°, indicating that ZMH has two polymorphic forms. Moreover, because of the strong adhesiveness (the crystal precipitated in 1M HNO3), it is important to keep the concentration of HNO3 at 3 M.

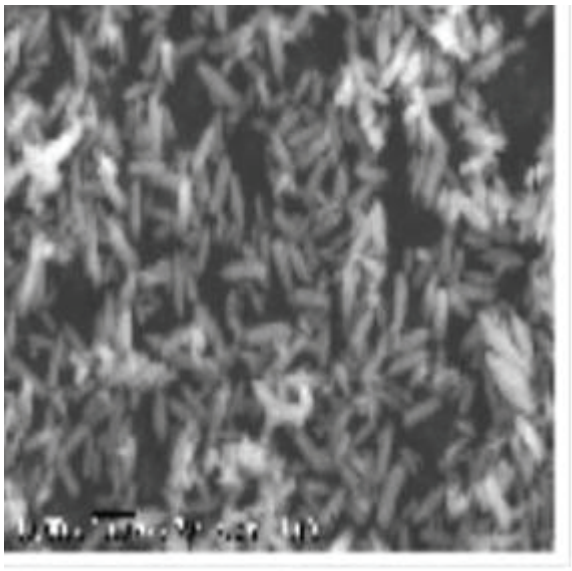

Fig. 4.6 SEM image of ZMH

(ZMH crystal precipitated in the concentration of 1N HNO_3)

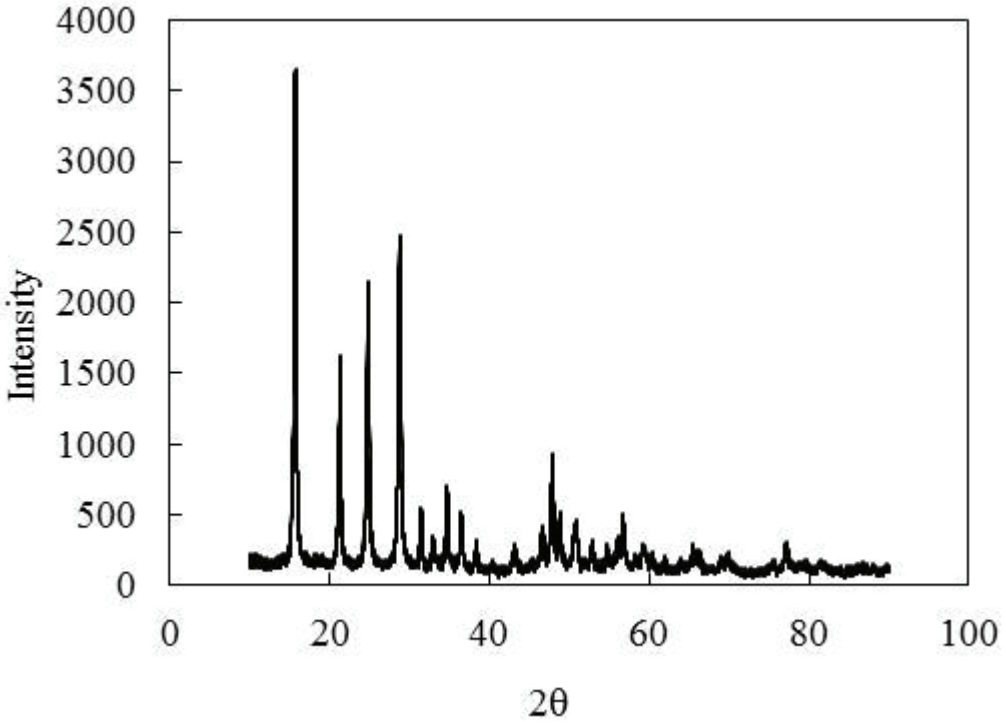

Fig. 4.7 XRD of ZMH(ZMH crystal precipitated in the concentration of 1N HNO_3)

4.3.3 Color changing of ZMH

As described in the experiment 2.2, two colors of ZMH precipitates (white and yellow) were observed while ZMH was crystallizing. For interpreting the mechanism for color changing of ZMH, the concentration of solution and the particle size were measured every 60 min after nucleated. As the result, it was observed that the mixed solution was suspension and white precipitates was sticking to the crystallizer for about 60 min. After then, yellow precipitates grew up on the surface of white precipitates. Yellow accumulation increased with the reaction time. Figure 10 shows the image of dry ZMH crystals. The color of 120 min crystal is stronger than that of 60 min crystal but there was no difference in XRD. On the next, the particle sizes of ZMH aggregate were measured. As shown in Fig. 11, ZMH has a wide CSD at the level of 0–40 μm. There is a strong peak at the seed size of 0–10 μm for white precipitates, but not for yellow precipitates. We reasoned that because of the growth of crystal, different light refractions would cause a color changing of ZMH. In addition, it became clear that white ZMH crystals were much easier to stick to crystallizer than to grow up. Therefore it is essential to reduce the amount of small ZMH crystals in a short time for preventing ZMH sticking.

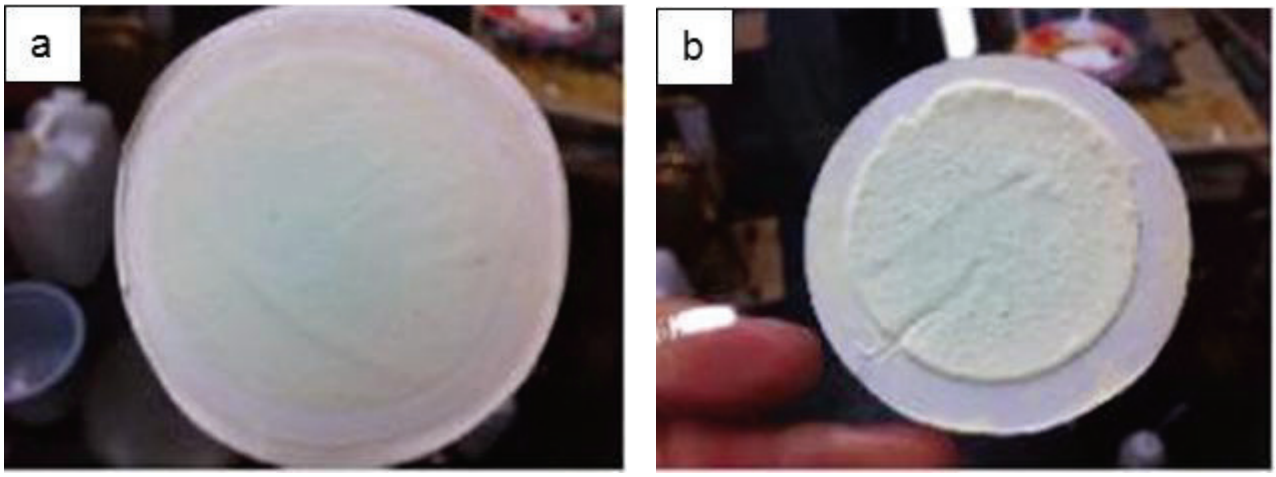

Fig. 4.8 Image of ZMH crystals

a: reaction time is 60 minutes. b: reaction time is 120 minutes.

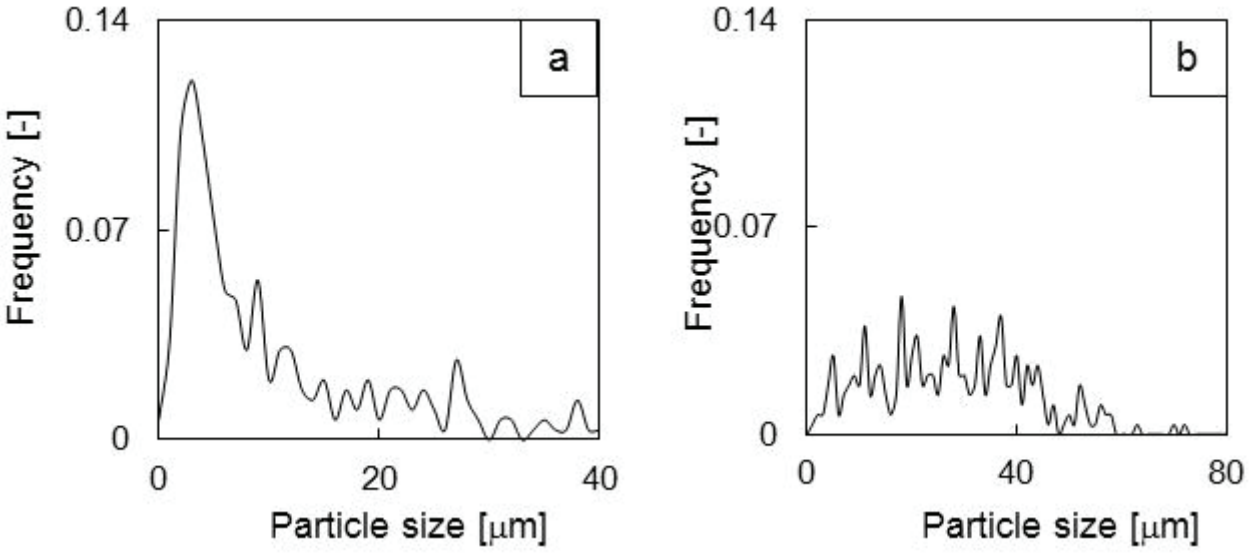

Fig. 4.9 CSD of ZMH in concentration of 3N HNO_3

a: reaction time is 60 minutes. b: reaction time is 120 minutes.

4.3.4 Preventing of ZMH encrustation by crystal growth

4.3.4.1 Batch crystallization method

Fig. 4 shows the SEM image of ZMH samples which were dehydrated for one day. At each nitric acid concentration and operating temperature the agglomeration was measured. And crystal shape changed with varying nitric acid concentrations and operating temperatures. In addition, mono dispersed particle were not observed.

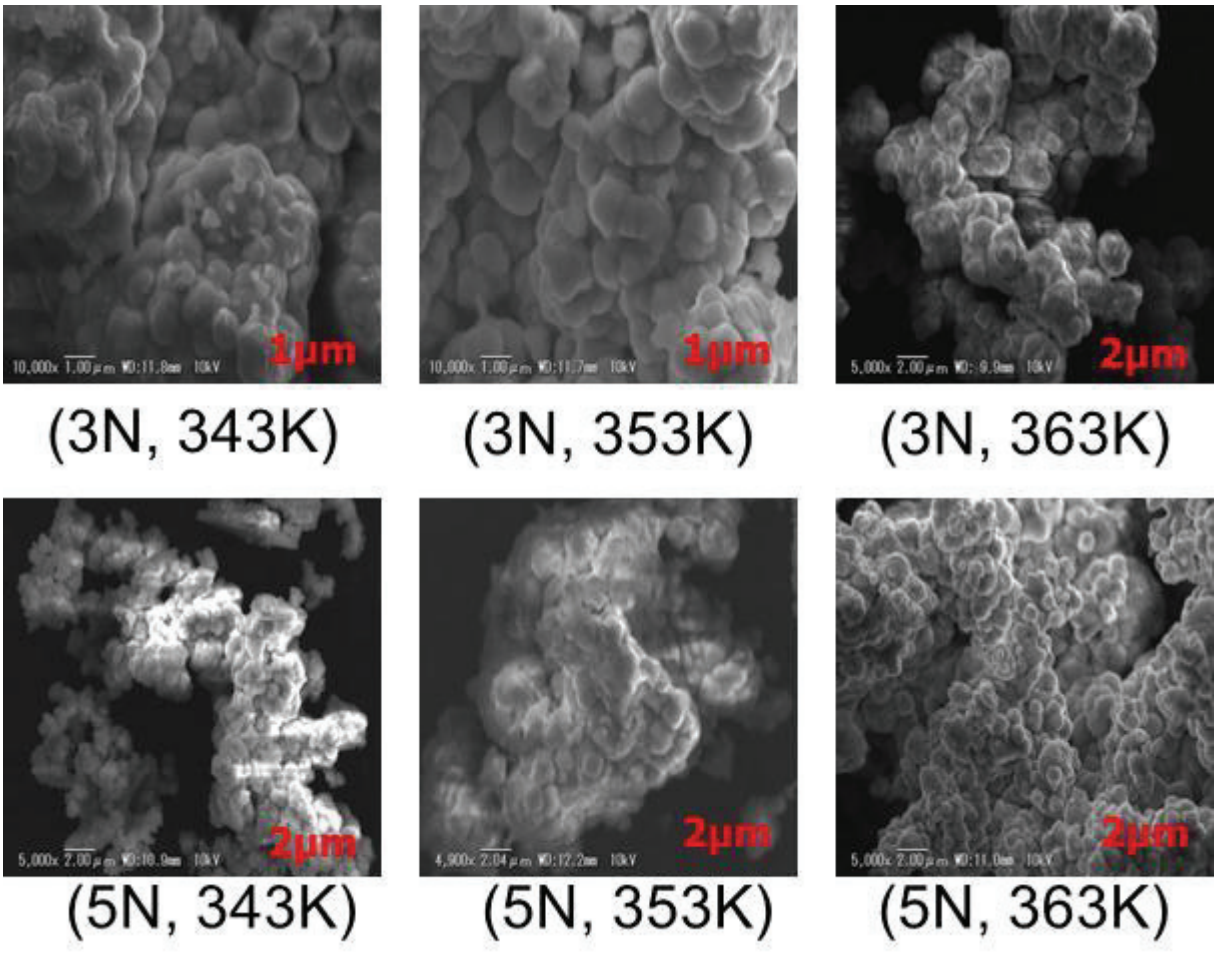

Fig. 4.10 SEM image of ZMH

4.3.4.2 The crystal size distribution of produced ZMH

Figure 6 shows the crystal size distribution (CSD) of ZMH particle. Despite the higher nitrate concentrations and operating temperatures, most of the data on average particle sizes produced by reactive crystallization scattered around 1 μm. After ZMH nuclearized, crystal growth stopped at 1 μm quickly, and then large amounts of small particles formed big agglomerate. The small ZMH particle was easily to stick on the crystallizer and also formed a big agglomeration. It can be considered that the concentration of nitric acid and temperature does not affect CSD of ZMH.

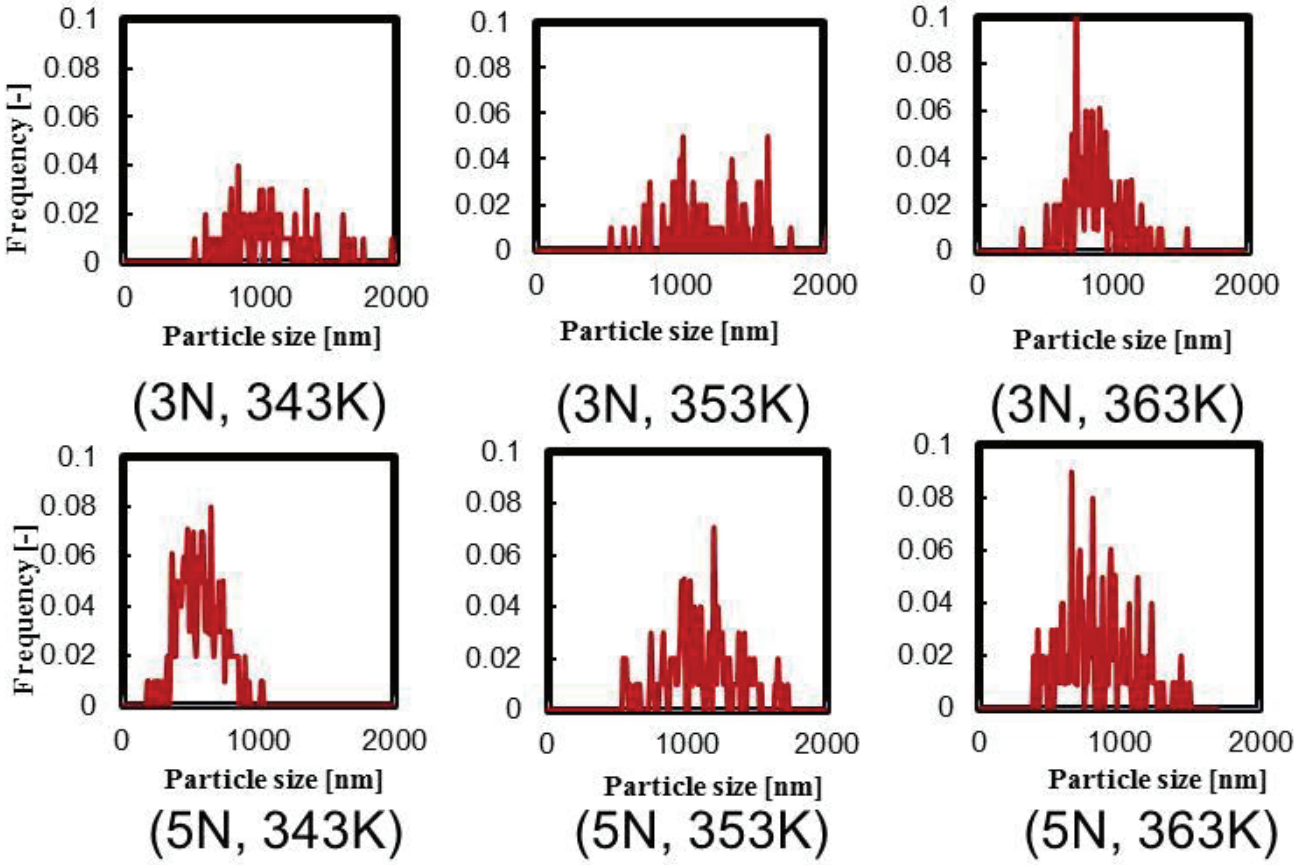

Fig. 4.11 CSD of ZMH

4.3.4.3 Single jet method

The SEM images of ZMH crystal at 90 degree Celsius are shown in Figure 3. (A) is the SEM image of ZMH crystals based on the batch method for 2 hours. The bar is 2□m. (B) is the SEM image of that based on the single

jet method for 2 hours. The bar is 4□m. (C) is the SEM image of that based on the single jet method for 6 hours. The bar is 2□m. As the changing from image (A) to (C), it was observed that the ZMH particles have a significant change from agglomeration to dispersion. Since Mo was added into the test tube slowly, the amount of fine ZMH particles which easily agglomerates with each other decreased in the solution. It is confirmed that (C) is ZMH by X-ray. X-ray chart is shown in Figure 4. Next, the concentration of ZMH solution plotted against time is shown in Figure 5. Round plots show the data from the single jet method for 2 hours. And tetragonal plots show the data from the single jet method for 6 hours. It is easy to know that the concentrations of single jet are higher than batch after the reaction, as Mo was added into the test tube slowly. According to this method, the growing up fine ZMH particles without agglomerating was achieved successfully in this study. In addition, it was observed that adherence of the ZMH on the inner surface reduced. The reason is that the adhesive power of ZMH became to be unable to support itself against the downward pull of its own gravity because the ZMH particle grew up to enough big size. The results would explain that the single jet method has a positive effect to prevent encrustation because of the particle growth of ZMH.

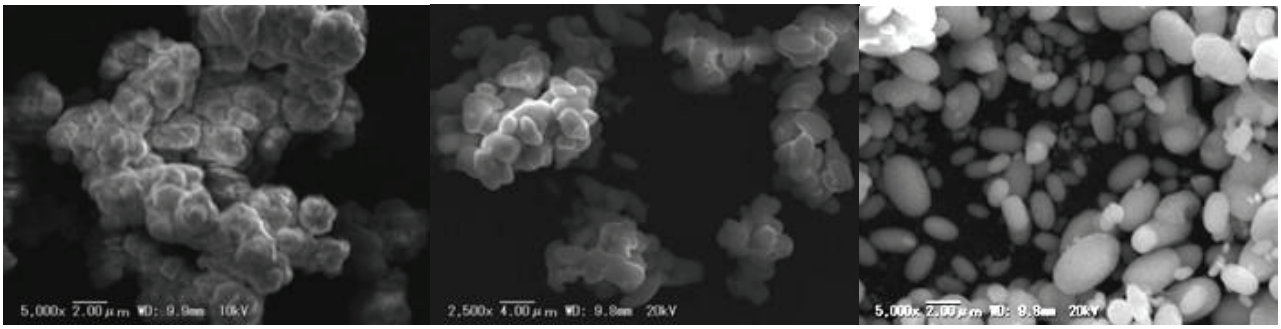

(A) (B) (C)

Figure 4.12 SEM image of precipitations from batch method and single jet method

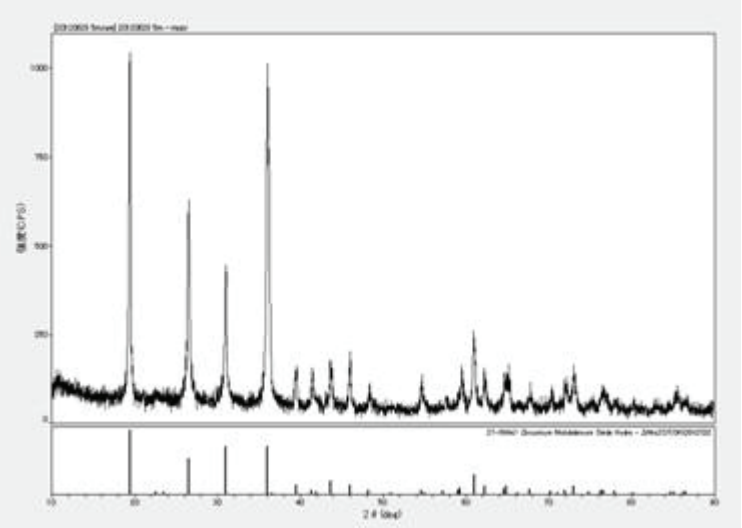

Figure 4.13 X-ray chart of ZMH with single jet method for 6hours

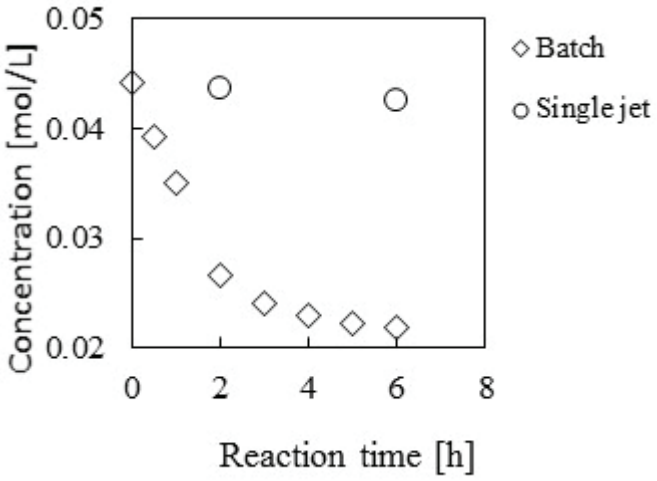

Figure 4.14 ZMH Concentration ploted against reaction time

(Batch and single jet method)

Conclusions

ZMH crystal could not grow up more than 1 μm, even though the concentration of nitric acid and temperature were varied. However, the ZMH crystal grows up as an aggregate with a wide particle size distribution. The color and adhesiveness of ZMH crystal are related to its particle size. It can be concluded that the control of nitric acid concentration and small particle growth would be the point to prevent ZMH sticking. Single jet method has a positive effect to prevent encrustation because of particle growth of ZMH.

Reference

1. Kubota M, Fukase T. Formation of precipitate in high-level waste from nuclear fuel reprocessing. Journal of Nuclear Science and Technology, 1980, 17(10): 783–790

2. Cansheng L. Study of precipitation behavior of Mo and Zr in nitric acid solution. Journal of Nuclear Radiochemistry, 1992, 14: 24–30

3. Doucet F J, Goddard D T, Taylor C M, Denniss I S, Hutchison S M, Bryan N D. The formation of hydrated zirconium molybdate in simulated spent nuclear fuel reprocessing solutions. Physical Chemistry Chemical Physics, 2002, 4(14): 3491–3499

4. Usami T, Tsukada T, Inoue T, Moriya N, Hamada T, Serrano Purroy D, Malmbeck R, Glatz J P. Formation of zirconium molybdate sludge from an irradiated fuel and its dissolution into mixture of nitric acid and hydrogen peroxide. Journal of Nuclear Materials, 2010, 402(2–3): 130–135

5. Magnaldo A, Masson M, Champion R. Magnaldo. Nucleation and crystal growth of zirconium molybdate hydrate in nitric acid. Chemical Engineering Science, 2007, 62(3): 766–774

6. Chater J. Waste not, want not: nuclear reprocessing and stainless steel. Stainl Steel Wold JST, 2005, 17: 42–47

7. Recktenwarld G D, Deinert M R. Cost probability analysis of reprocessing spent nuclear fuel in the US. Energy Econ JST, 2012, 34(6): 1873–1881

8. Baja B, Varga K, Szabó N A, Németh Z, Kádár P, Oravetz D, Homonnay Z, Kuzmann E, Schunk J, Patek G. Long-term trends in the corrosion state and surface properties of the stainless steel tubes of steam generators decontaminated chemically in VVER-type nuclear reactors. Corrosion Science, 2009, 51(12): 2831–2839

9. Matsumura K, Kawamura W, Miyake T. JP Patent, 2000-56077(2000.02.25)

Chapter5

Encrustation preventing on seed addition

5.1 Introduction

In the nuclear electric power generation, a variety of impurities is produced by uranium fuel nuclear fission reaction [1]. In the dissolution step of the nuclear fuel waste, there are world-concern problems that zirconium molybdate (ZMH) precipitated as a byproduct, accumulated in the reactor [2, 3, 4]. Then nucleation and crystal growth of zirconium molybdate hydrate in nitric acid was discussed [5]. In order to remove the accumulation, various physical and chemical cleaning methods have been discussed; however, they were also accompanied by new problems because of their disadvantages. For examples, if using the high pressure water to remove the accumulation, workers are at risk of being exposed to radiation when they enter into the device; if using high concentrations of acid or alkaline for a long time, the reactor and pipes would be corroded. Moreover, a new method has been succeeded in preventing accumulation. JAEA reported that little accumulation was observed in the reactor when small round zirconium metals were added since it is easier for the major component of accumulation ZMH to stick on the surface of the zirconium metal rather than the reactor. However, this method is expensive and difficult in reuse. [6]

In this study, in order to prevent accumulation, a new method based on crystallization engineering was proposed. This method is based on the control of crystallized reaction of zirconium molybdate in the waste solution, followed by a solid-liquid separation. In the first step, in order to measure the particle size of ZMH, batch crystallization experiments were conducted by varying nitric acid concentration and operating temperature. In result, almost all particle sizes scatter around 1 μm on average, despite the higher concentration of nitric acid and operating temperature, and then small particles grow up as an aggregate sticking to the crystallizer. [7] Next, to observe zirconium molybdate sticking on the reactor, batch crystallization experiments were conducted by varying operating temperature. Using the result, exponent of supersaturation was calculated. Based on these results and after consulted plenty of scaling processes of other materials [8-11], we have had a conception that fine ZMH particle is easy to stick to the inner face of the reactor, so absorb the fine particles would be very important for preventing the ZMH accumulation. Therefore, in order to prevent ZMH accumulation, seed additive experiments were conducted by varying the crystal seed sizes. However, there are still some problems not clear about this study, for example, why does the concentration of Mo fall below that of Zr in a higher concentration of nitric acid solution than 3M. In this report, these problems were discussed and the advanced

encrustation preventing method was proposed.

From what has been mentioned above, seeding policy to prevent encrustation of zirconium molybdate is suggested by considering the seeding size and added amount. According to the observation, ZMH turned to be bigger than its original size after the reaction, as it absorbed the ZMH to stick on itself instead of the surface of beaker. As far as I am concerned, new seeding policy could solve the problem on zirconium molybdate encrustation in the process of dealing with nuclear fuel waste, and detailed research on nucleation and growth kinetics is still necessary for further study.

5.2 Experimental Methods

In nitric acid, zirconium molybdate was produced with the reaction of sodium molybdenum (VI) dihydrate and zirconyl nitrate dehydrate. The mechanism of reaction is shown as expression (2.1).

$$2HMoO_4^- + ZrO_2^+ + 2H_2O \rightarrow Zr(OH)_2Mo_2O_7(H_2O)_2 \quad (2.1)$$

5.2.1Materials

Molybdenum(VI) in nitric acid (from 61.3% nitric acid, Wako, Japan) was prepared by dissolving Sodium molybdate dihydrate ($Na_2MoO_4 \cdot 2H_2O$, Wako, Japan). Zirconium(IV) in nitric acid was prepared at by dissolving reagent grade zirconyl nitrate dihydrate ($ZrO(NO_3)_2 \cdot 2H_2O$, Wako, Japan). Mixing this Molybdenum and Zirconium solution, the concentration of Molybdenum became 0.1mol/L, and the concentration of Zirconium became 0.05mol/L. And the concentration of nitric acid of this mix solution was prepared at 3M.

5.2.2 Effect of operating temperature on adhesiveness of ZMH

First, the mix solution (from 2.1) 50ml was prepared in a reactor. Second, operating temperatures, were varied from 70 to 100 degree Celsius. At every operating temperatures, Zirconium Molybdate was crystalized, Figure 1. When the reaction finished, yellow precipitation and white precipitation was separated, then samples were made. After that ZMH crystal samples were dehydrated for one day. After dehydrating, the ZMH crystal samples were observed by Scanning Electron Microscopy (SEM).

5.2.3 Variation of concentration of ZMH solution with time

First, the mix solution (from 2.1) 50ml was prepared in a reactor. Second, operating temperatures, were varied from 70 to 100 degree Celsius. At every operating temperatures, Zirconium Molybdate was crystalized, Figure 1. Solution samples were taken at 0, 0.5, 1, 2, 3, 4, 5, 6 hour after ZMH nucleated. Then the concentration of samples was measured by Inductively Coupled Plasma- Mass Spectrometry (ICP-MS).

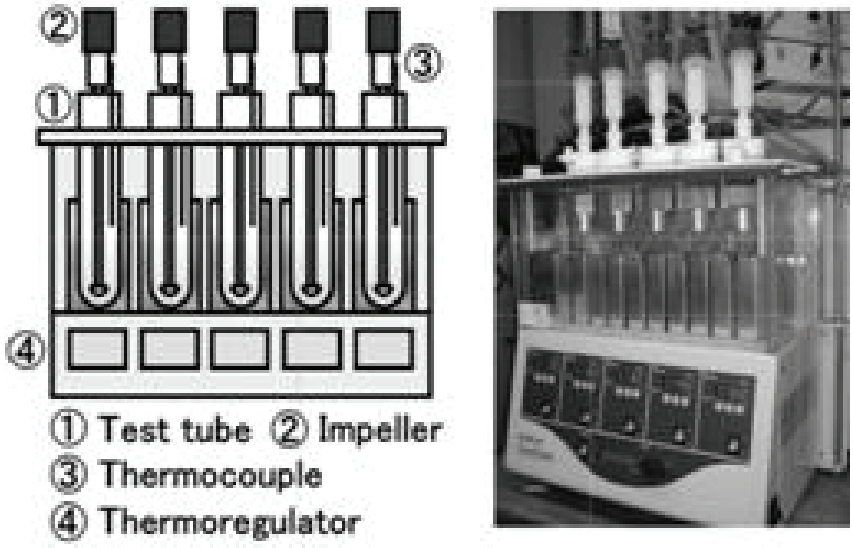

Figure 5.1 Experimental apparatus

5.2.4 Preventing ZMH sticking by seed additive

The mix solution (from 2.1) 100ml was poured into a reactor. ZMH crystal seeds (particle sizes were 10, 37.5, 50 □m) were added with different weights (3.5-9 g). At each concentration of nitric acid, Zirconium Molybdate (ZMH) was crystallized at the same condition, operating temperature was 90 degree Celsius and the concentration of nitric acid was 3M. Next, ZMH crystals were dehydrated for one day. After dehydrating, property of the ZMH crystals were analysed by Scanning Electron Microscopy (SEM). As another experiment, ZMH crystal seed addition experiment, particle size of seeds was 10 μm, was conducted. With the same method, Zirconium Molybdate (ZMH) was crystallized at 90 degree Celsius, Amount of seeds, Table 1, were varied from 2 to 3.1 g.

Table 5.1 Experimental condition

Concentration of $ZrO(NO_3)_2 \cdot 2H_2O$	[mol/L]	0.05
Concentration of $Na_2MoO_4 \cdot 2H_2O$	[mol/L]	0.1
Concentration of HNO_3	[mol/L]	3
Reaction time	[hr]	2
Reaction temperature	[degree Celsius]	90
Amount of seeds	[g]	2, 2.8, 3, 3.1

5.2.5 Discussion about the by-product over ZMH precipitation

The 50 ml of mix solution (from 2.1) was prepared in a test tube. The operating temperatures were varied from 70 to 100 degree Celsius. At every operating temperature, the ZMH was crystallized in the test equipment as shown in Figure 2 for 2 and 24 hours. When the reaction finished, yellow precipitation and white precipitation was separated and sampled. Next, the ZMH crystal samples were dehydrated for one day. After dehydrating, they were observed by Scanning Electron Microscopy (SEM), Raman spectroscopic analysis and X-radiation. Finally, molar ratio of Mo/Zr on the ZMH crystal samples, which were dissolved in 95% sulfuric acid at 270 degree Celsius, was measured by Inductively Coupled Plasma- Mass Spectrometry (ICP-MS).

5.3 Results and Discussion

5.3.1 Preventing ZMH sticking by varying operating temperature

With 24 hours reaction, there were white and yellow stickings on the inner surface of all of the text tubes, varying operating temperature at the range of 70-100 degree Celsius. The higher operating temperature is increased, the more ZMH crystallized. White sticking is easy to be cleaned off from text tubes by ultrapure water at higher operating temperature. Figure 2 shows the image of the reactor with a 24h reaction. From the left side, the operating temperature is 70, 80, 90 and 100 degree Celsius. About 70 degree Celsius sample, yellow precipitation was easy to clean, but white precipitation strongly sticked to the crystallizer. On the other hand, about 100 degree Celsius sample, more than half of the white precipitation was dropt by ultrapure water cleaning. As the result, it is considered that adhesive force of white sticking got to be unable to support itself against the downward pull of its own gravity when ZMH agglomeration got bigger on the surface of white sticking at high superseturation.

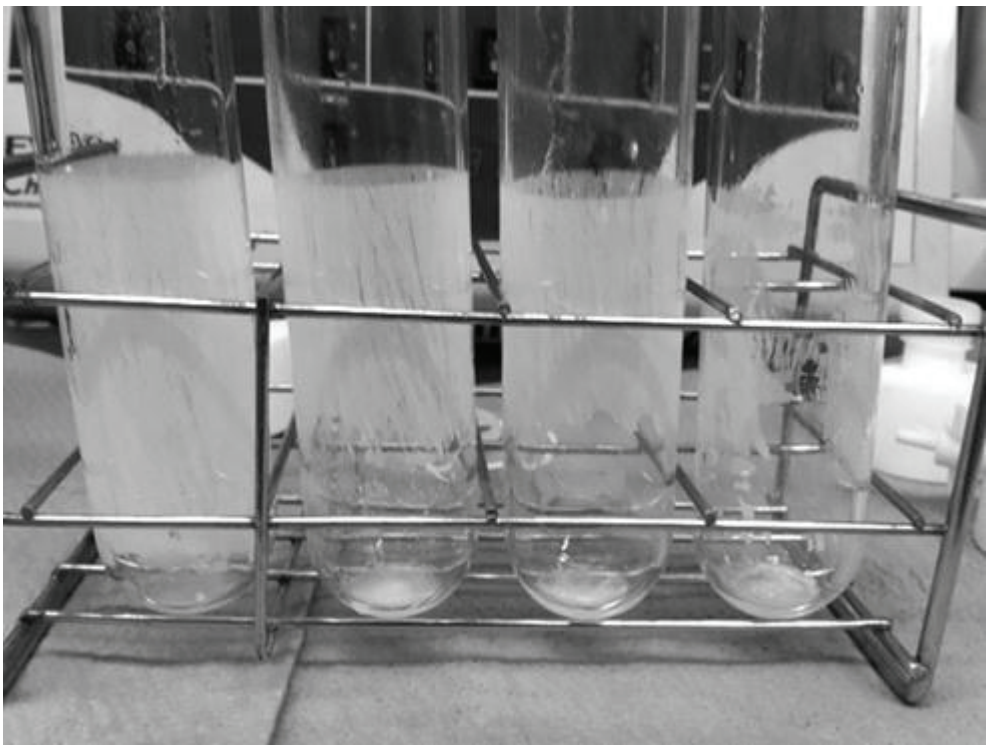

Figure 5.2 Observed white sticking on the crystallizers

5.3.2 Observation of white precipitation by SEM

ZMH white precipitation was observed by SEM in this experiment. Figure 3 shows the SEM image of ZMH white precipitation appeared on the inner surface of the text tubes. Image A: side face of white precipitation at 70 degree Celsius. The length of the bar is 3.03 □m. Image B: side face of white precipitation at 100 degree Celsius. The length of the bar is 4.00 □m. Image C: surface of white precipitation contacted with crystallizer at 70 degree Celsius. Image D: surface of white precipitation contacted with crystallizer at 100 degree Celsius. About image A and B, it is observed that small ZMH particles (about 1 □m) agglomerate into white sticking. Thickness of the white is about 2-3 μm. And the thickness would not change by varying operating temperature. In addition, two different surfaces of the white sticking can be observed: one with a tightly bonded structure appeared on the inner surface of the beaker; on another one, ZMH crystal grew up in an inhomogeneous manner [7]. C and D show the different status of the surface of white sticking. C has a tightly bonded structure in gradual nucleation at low operating temperature. Countering to that, D has a concave-convex structure in combative nucleation at high operating temperature. Therefore, adhesive force of white sticking got to be unable to support itself against the downward pull of its own gravity when contact area reduced with a concave-convex structure. It would be considered that operating temperature control is useful to prevent ZMH accumulation.

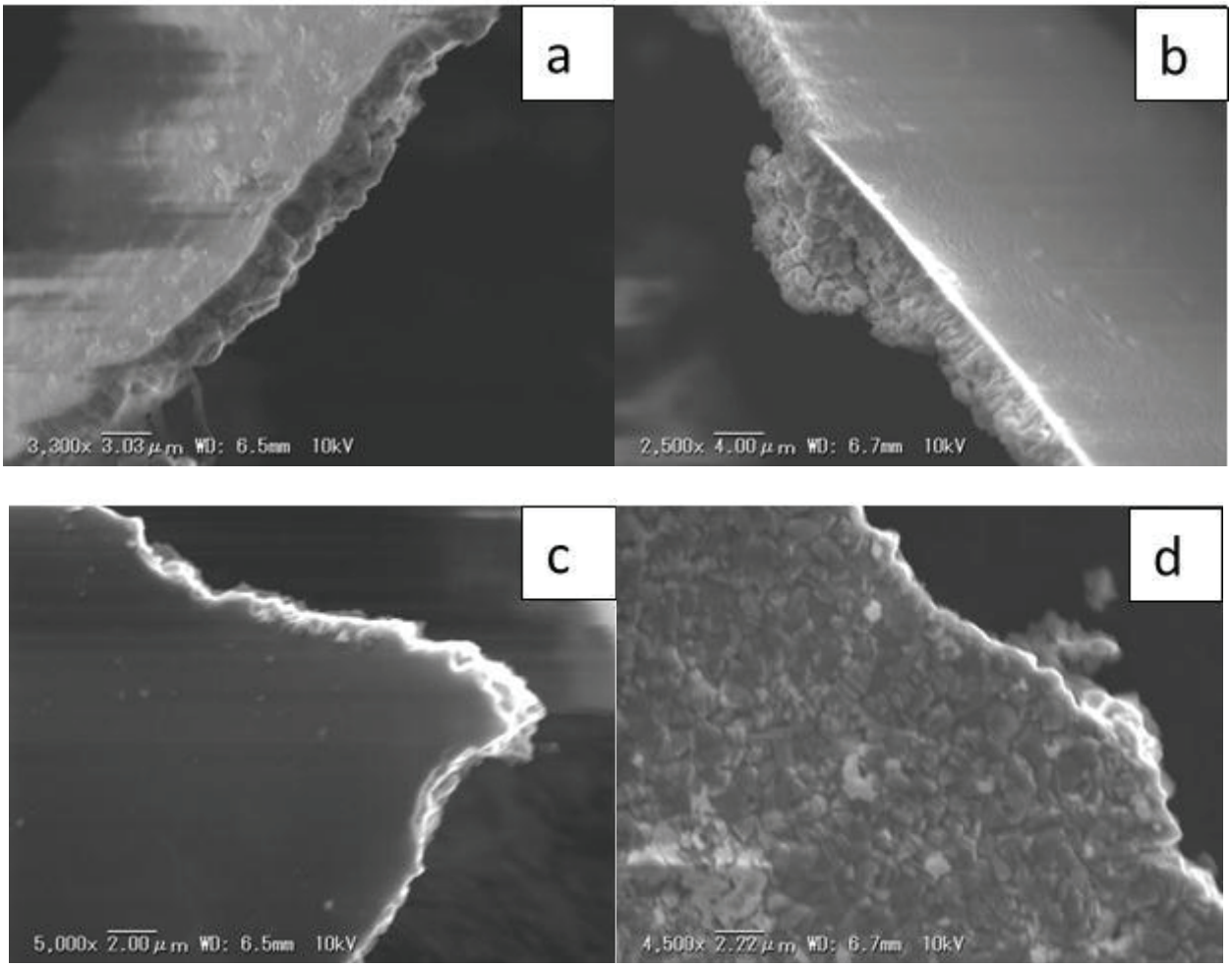

Figure 5.3 SEM image of ZMH white precipitation

5.3.3 Crystal seed addition

At the first step of seed addition experiment, to absorb the fine ZMH particle which nucleated over the reaction, rate of nucleation of ZMH was discussed. Figure 4 shows the concentration of ZMH solution plotted against the reaction time. The concentration reduces with nucleation becomes faster since the operating temperature is increased. The concentration reduces fast within 2 hours, then the variation of it becomes slowly. Therefore, it is important to absorb the fine particle of ZMH which nucleated within the first 2 hours.

Next, for preventing ZMH sticking, effect of seeding was discussed. Because of the small particle, ZMH was easy to stick on the crystallizer or become to a big agglomeration. For this reason, it is considered that it was easier to stick to itself than the surface of reactor when ZMH crystal seeds were added into the reaction vessel. Figure 5 shows the image of ZMH sticking on the surface of the reactor. As a consequence, when the crystal

seeds of particle size 50 □m were added by 9 g, zirconium molybdate sticking was not observed on the beaker any more. Following the quality of ZMH crystal seed increased, surface area of ZMH crystals increased. So it is easy to consume the small particles, and prevented ZMH sticking. As the same way, when the 37.5 □m crystal seeds were added by 7 g, and the 10 □m crystal seed was added by 3.5 g, the same phenomenon could be observed.

As the results of varied operating temperature in the range of 70-100 degree Celsius, white sticking was not observed on the inner face of the text tubes after 2 hours reaction when 10 □m ZMH seeds were added by 2, 2.8, 3, 3.1 g at each operating temperature, as showing in Figure 6. Figure 7 shows the mass of sticking per superficial area of reactor plotted against the supersaturation of solution per surface area of seed crystals. The surface area of seed crystals increases with increasing fine particles since the superaturation level is increased. It is considered that the higher operating temperature is increased, the larger surface area of seed is requested to absorb the fine particles which stick to the inner surface of text tube and start growing. Based on the results, a new experiment about discussing the quantity of white sticking was conducted. Fixed the quantity of seed additive, ZMH was crystallized for 2 hours by varying the operating temperature, and the other experimental parameters were the same as 2.4. As the results, the mass of sticking per surface area of reactor plotted against the supersaturation of solution per surface area of seed crystals was shown in Figure 8. From these results, amount of seed additive can be easily to be calculated by supersaturation of ZMH solution, and it is also possible to check the quantity of sticking on the inner face of reaction without enough seed additive.

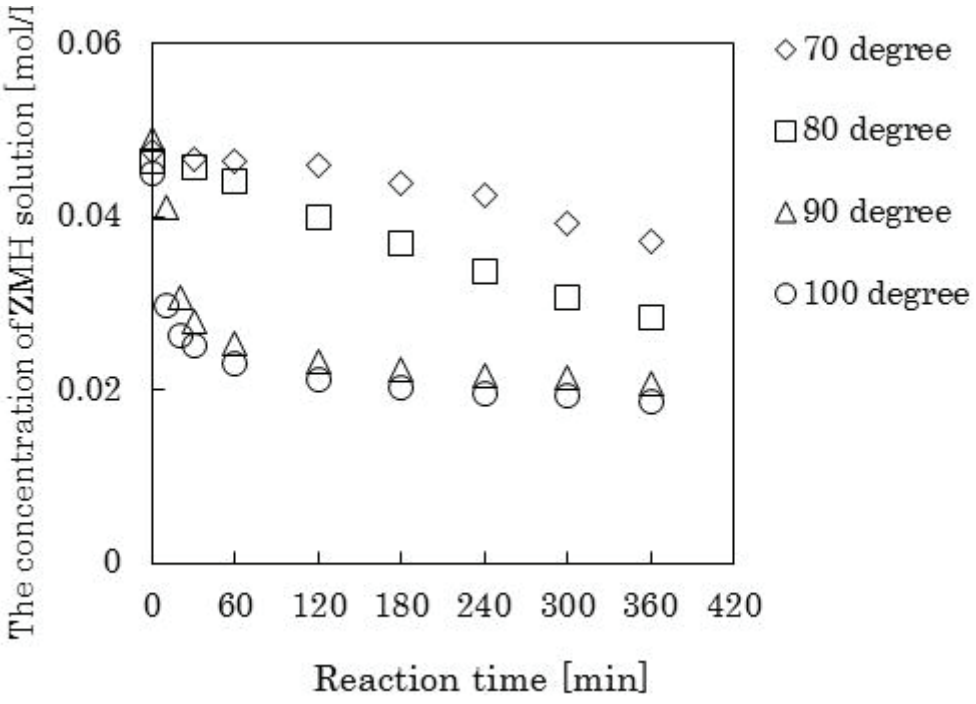

Figure 5.4 the concentration of ZMH solution plotted against the reaction time

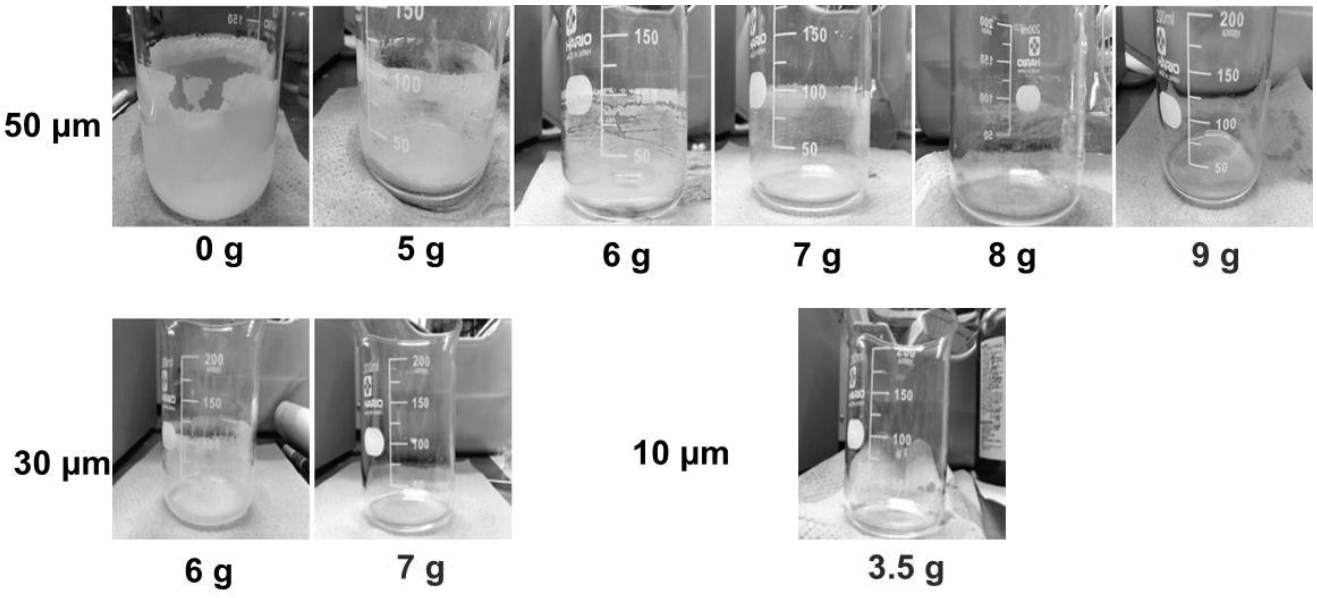

Figure 5.5 Observed ZMH sticking on the surface of the reactor

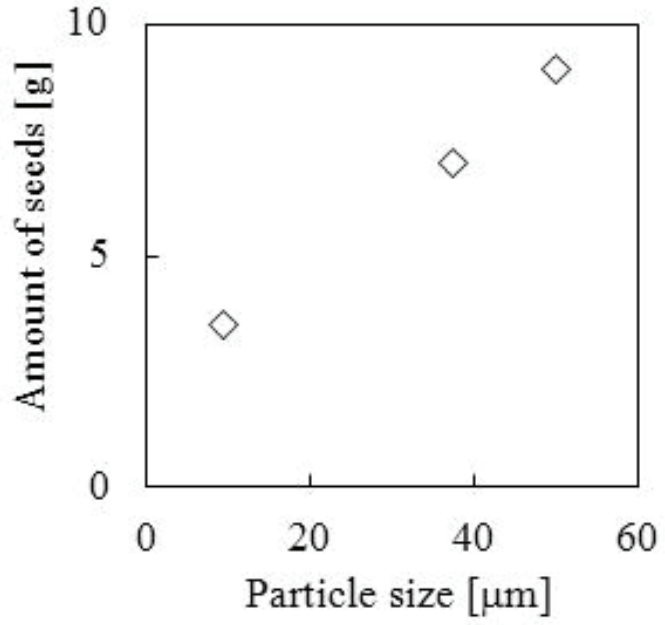

Figure 5.6 Seed mass fraction and seed size to prevent ZMH accumulation

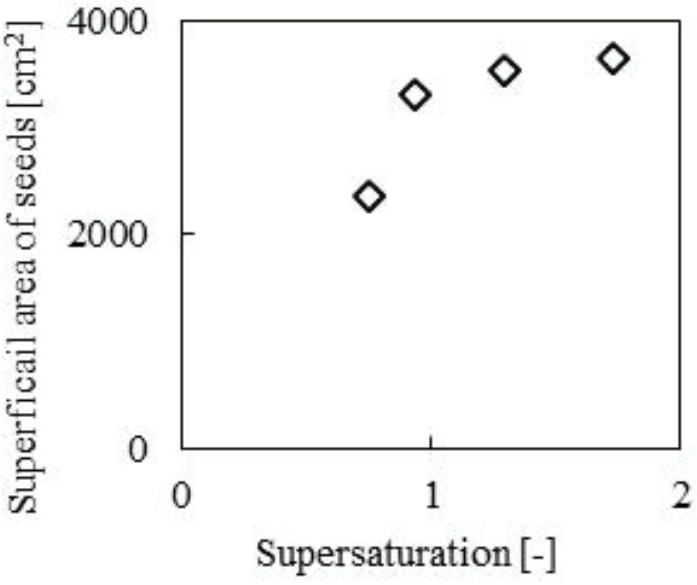

Figure 5.7 Surface area of seeds plotted against supersaturation

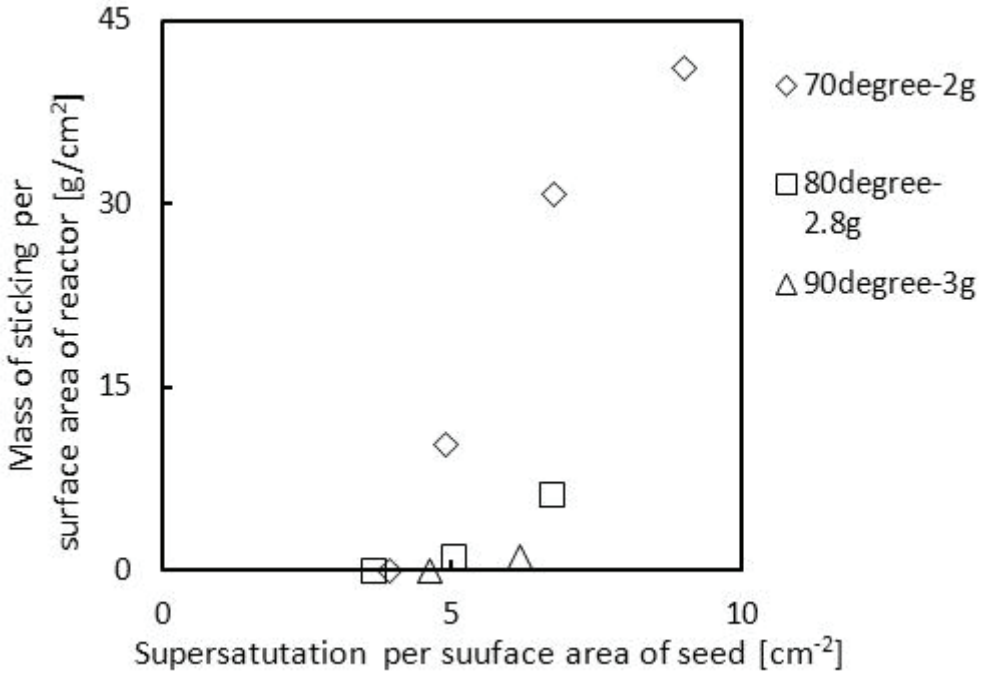

Figure 5.8 Variation of sticking on the reaction with operating temperature

5.3.4 Discussion about the by-product over ZMH precipitating

In the precious step of this study, there was an opposite result to the original expectations. ZMH solution should keep the molar ratio, since ZMH crystal precipitated as a molar ratio (Mo/Zr=2) in the solution which is prepared as a molar ratio (Mo/Zr=2). However the solubility of Mo fell below that of Zr in nitric acid solution when the concentration of nitric acid was varied from 3M to 5M (Zhang et al., 2013). In this experiment, the reason of the results is that the concentration of Mo decreased as variation of concentration of nitric acid was discussed. Molar ratio (Mo/Zr) plotted against operating temperature is shown in Figure 7. With a 24hours reaction the molar ratio (Mo/Zr) dropped to less than 2 in each experimental condition. In the same concentration of nitric acid and reaction time, the molar ratio (Mo/Zr) decreased with increasing amount of precipitation since the operating temperature was increased. Compared with the result of 2hours, the molar ratio (Mo/Zr) decreased with a 24hours reaction. Compared with 3M, the molar ratio (Mo/Zr) of 5M nitric acid decreased. As the results, it is possible that an unknown by-product which has a molar ratio (Mo/Zr) more than 2 precipitated over ZMH composition. Based on the molecular structure of ZMH (Clearfield et al., 1972) in Figure 6, Zr-O-Mo bond is easy to be broken down in a nitric acid solution with higher concentration.

Next, the ingredients of crystal which sticked on the inner surface of the text tubes (3, 5M nitric acid, 24hours reaction) were measured, as shown in Figure 8. In each experimental condition the molar ratio of Mo/Zr exceeded 2. In agreement with Figure 7, the molar ratio (Mo/Zr) in 5M nitric acid is larger than that in 3M. Compared with the crystals in the solution, the molar ratio (Mo/Zr) of crystal which sticked on the inner face of the test tube becomes larger. As the results, it is possible that the by-product is also easy to stick on the inner face of the test tube.

Based on the results of chapter 3.1, a qualitative analysis of by-product was conducted by varying the concentration of nitric acid in the range of 5-9M. Raman spectroscopic analysis of crystal, sticking on the inner face of the test tube, is shown in Figure 9. Raman spectroscopic analysis of the crystals in 5 and 7M has the same chart. The peak of ZMH around 850 [cm^{-1}] and the peaks of $ZrMo_2O_8$ around 700 and 950 [cm^{-1}] were detected. $ZrMo_2O_8$ may be produced by the heat of laser during Raman spectroscopic analysis. In 9M, the peaks of ZMH and $ZrMo_2O_8$ and several unknown peaks around 100-200 [cm^{-1}] were detected as well. Next, XRD chart of crystal, sticking on the inner face of the test tube in 9M, is shown in Figure 10. The peaks both of ZMH and

molybdenum trioxide hydrate were detected. As the results, it is clear that the by-product is molybdenum trioxide hydrate. Based on Figure 8, by the reason of that molybdenum trioxide hydrate is easy to stick on the surface of the test tube, it is important to add more seeds to absorb both fine ZMH and molybdenum trioxide hydrate particles in the solution for preventing encrustation.

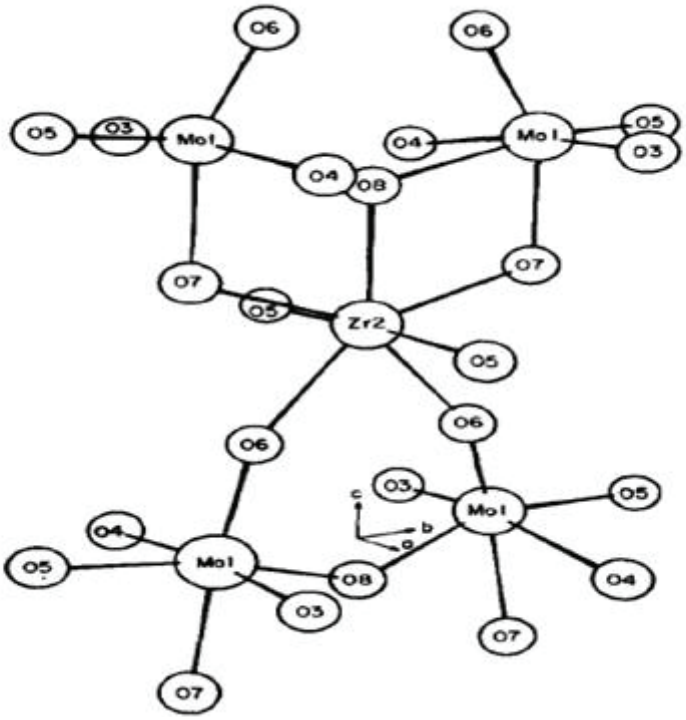

Figure 5.9 molecular structure of ZMH (Clearfield et al., 1972)

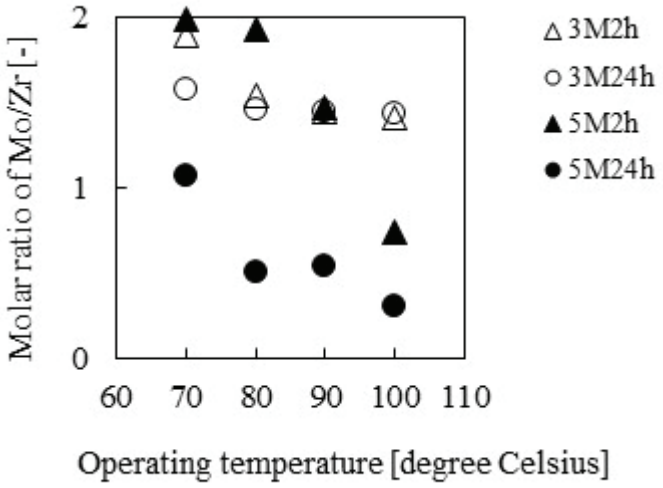

Figure 5.10 Molar ratio of Mo/Zr plotted against operating temperature

(crystals in the solution)

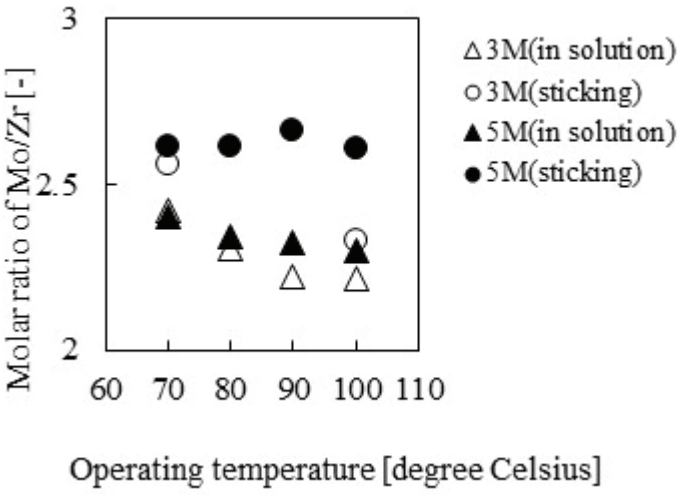

Figure 5.11 Molar ratio of Mo/Zr plotted against operating temperature

(sticking on the surface of test tube)

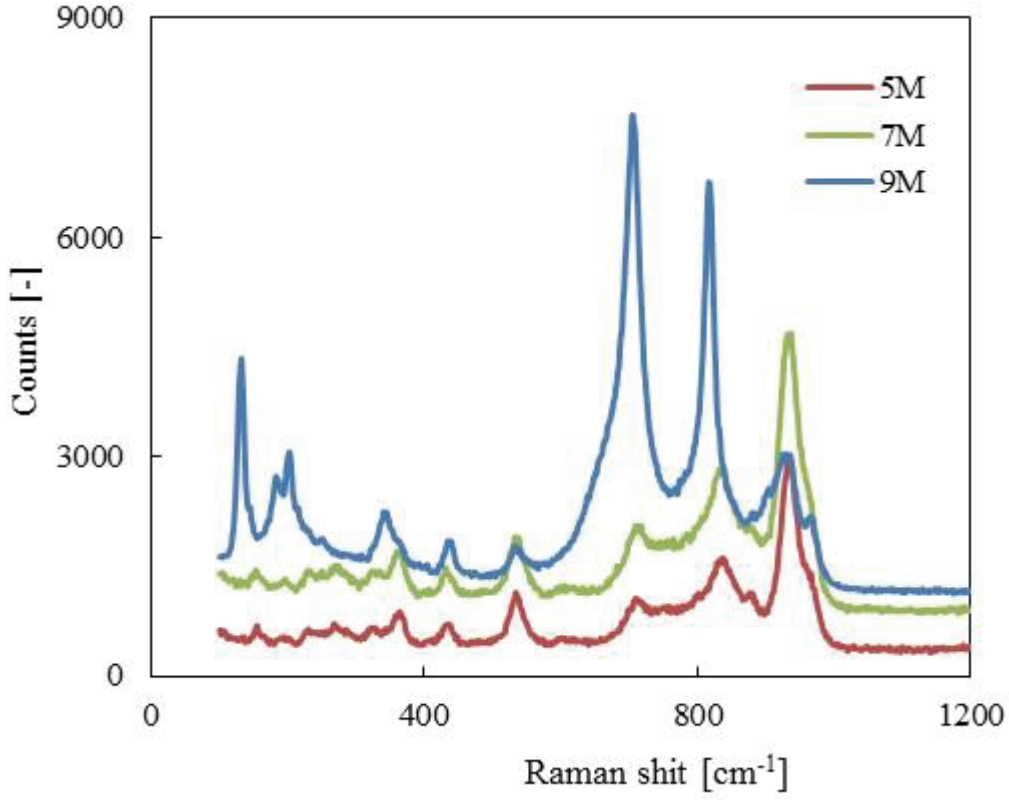

Figure 5.12 Raman spectroscopic analysis of crystal sticked on the inner surface of the test tube

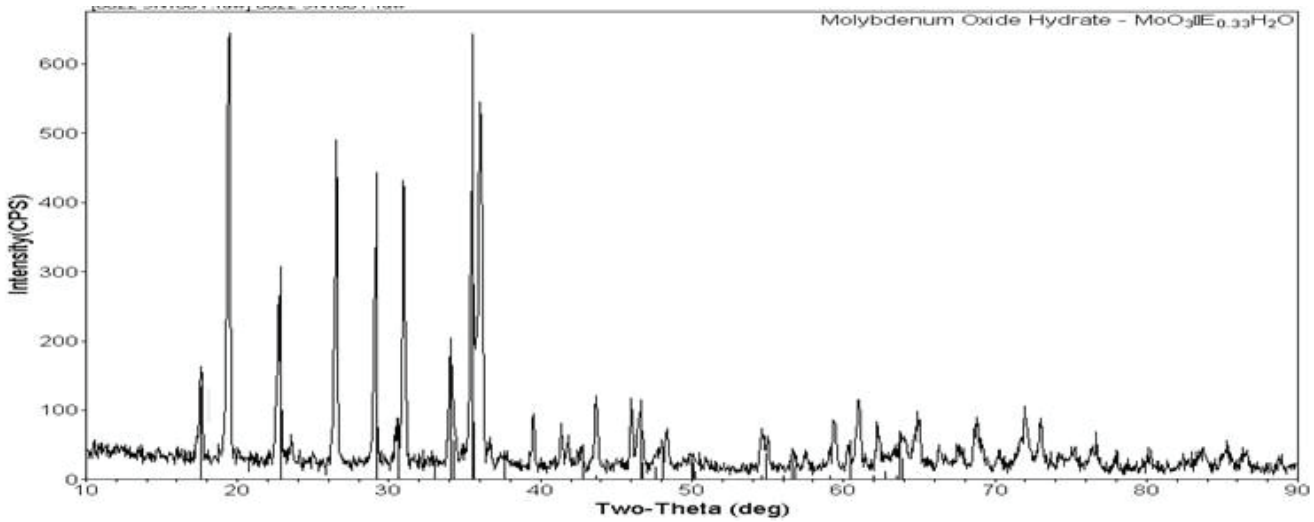

Figure 5.13 X-ray chart of crystal sticked on the inner surface of the test tube

Conclusions

It is important to absorb the fine particle of ZMH which nucleated within the first 2 hours for preventing ZMH sticking and accumulation.From the results of this study, amount of seed additive can be calculated by supersaturation of ZMH solution.ZMH seed additive and temperature control are both efficient methods for preventing ZMH sticking and accumulation.

As the x-ray result, by-product is molybdenum trioxide hydrate.It is necessary to add more seeds to absorb both fine ZMH and molybdenum trioxide hydrate particles in the solution for preventing encrustation.

Reference

[1] Kubota, M., Fukase, T., Formation of precipitate in high-level waste from nuclear fuel reprocessing. Journal of Nuclear Science and Technology, 1980, 17, 783–790.

[2] Cansheng, L., et al., Study of precipitation behaviour of Mo and Zr innitric acid solution. Journal of Nuclear Radiochemistry, 1992, 14, 24–30.

[3] Doucet, F.J., The formation of hydrated zirconium molybdate in simulated spent nuclear fuel reprocessing solutions. Physical Chemistry and Chemical Physics, 2002, 4, 3491–3499.

[4] T. Usami, Formation of zirconium molybdate sludge from an irradiated fuel and its dissolution into mixture of nitric acid and hydrogen peroxide, Journal of Nuclear Materials, 2010, 402,130–135

[5] A. Magnaldo, Nucleation and crystal growth of zirconium molybdate hydrate in nitric acid, Chemical Engineering Science, 2007, 62, 766 – 774

[6] Matsumura K., Kawamura W., Miyake T., Japan Patent Kokai 2000-56077 (2000.02.25).

[7] Liang Z., Masayuki T., Tsutomu K., Izumi H., Evaluation of precipitation behacior of zirconium molybdate hudrate, Front. Chem. Sci. Eng., Vol. 7(1), 65-71(2013)

[8] Ingrida B., et al., Increasing conversion in membrane filtration systems using a desupersaturation unit to prevent scaling, Desalination, 119(1998)119-204

[9] John J. et al., A review of salt scaling: I. Phenomenology, Cement and Concrete Research, 37(2007)1007-1021

[10] Baoxia Mi, et al., Silica scaling and scaling reversibility in forward osmosis, Desalination, 312(2013)75-81.

[11] P. A. Kryukov, E. G. Larionov, Physico-Chemical Samling of High Temperature Wells in Connection with Their Encrustation by Calcium Carbonate, Geothermics, 1970. Vol. 2-2

[12] Clearfield, A. and R. H. Blessing; ‘‘The preparation and crystal structure of a basic zirconium molybdate and its relationship to ion exchange gels,’’ *J. inorg, nucl. Chem.*, **VoL 34**, pp. 2643-2663 (1972)

Chapter6

Conclusions

In this Ph.D. thesis, the author focuses on studies of the reaction crystallization which is widely used as a separation process in various industries. Reaction crystallization and seeding crystallization were investigated because these processes play an extremely important role to produce high-quality product in industry and the further technological development has been increasingly required due to the needs of higher specification. This study provides the fundamental data to clear the mechanism on some parts of reaction crystallization and suggests novel technological theories to support the practical application to the industrial crystallization processes.

In chapter 4, ZMH crystal could not grow up more than 1 μm, even though the concentration of nitric acid and temperature were varied. However, the ZMH crystal grows up as an aggregate with a wide particle size distribution. The color and adhesiveness of ZMH crystal are related to its particle size. It can be concluded that the control of nitric acid concentration and small particle growth would be the point to prevent ZMH sticking. Single jet method has a positive effect to prevent encrustation because of particle growth of ZMH.

In chapter 5, from the results of this study, amount of seed additive can be calculated by supersaturation of ZMH solution. ZMH seed additive and temperature control are both efficient methods for preventing ZMH sticking and accumulation.It is important to absorb the fine particle of ZMH which nucleated within the first 2 hours for preventing ZMH sticking and accumulation. More ever, as the x-ray result, by-product is molybdenum trioxide hydrate. It is necessary to add more seeds to absorb both fine ZMH and molybdenum trioxide hydrate particles in the solution for preventing encrustation.

Furthermore, the mechanism of precipitation behavior of the ZMH was illustrated. By interpreting aging variation of concentration, at the condition of growth and pleomorphism, it would be clear that how to prevent the ZMH sticking without using the cleaning media which includes any other materials. This new method for cleaning zirconium molybdate sticking would solve the problem in waste water treatment and resources recovery. Meanwhile, the detailed researches on nucleation and growth kinetics are still necessary for further study.

謝辞

本論文は、筆者が早稲田大学大学院先進理工研究科に在学中、博士後期課程の研究成果をもとに作成したものであります。本論文を作製するにあたり、指導教授であると同時に本論文の主査でもある平沢泉教授には懇切丁寧なご指導を賜りまして、深く御礼申し上げます。筆者は学部 4 年から化学工学の研究室に配属されて以来、一途に化学工学を研究してきました。専門知識を深く理解していくにつれ、博士課程から平沢教授におかれましては、研究面のご指導はもとより私生活に至るまで、幅広く色々な場面でご支援を賜りました。先生のご指導は、非常に優しさと暖かみにあふれており、多くの薫陶を受けました。間近で眺める先生のお姿は、研究者として、人間として、自分が自身の人生をどのように切り拓いていくかについて影響を与えて下さった師の鑑でした。ここより感謝し厚く御礼申し上げます。本論文を副査下さいました野田優教授、Halle wittenberg Martin-Luther 大学の Joachim Ulrich 教授には、研究のご指導を賜るだけでなく、化学工学会誌の編集委員会や国際学会 BIWIC など大学以外の仕事場におかれましても暖かく見守り、素晴らしい仕事姿を拝見させて下さったことに深く感謝申し上げます。また、酒井研究室に所属していた時からも大変お世話になりました小堀深講師はから賜った化学工学の視点に基づくご指摘は研究を進める上で貴重なものになりました。深く御礼申し上げます。

晶析分科会や化学工学会、分離技術会など学会や講演会にて貴重なご助言、ご指摘下さいました先生方に、厚く御礼申し上げます。その中でも豊倉賢早稲田大学名誉教授に特別温かいお言葉を掛けてくださいました事に感謝申し上げますと共に、研究室 OB の先輩方に感謝申し上げます。

研究面で大変お世話になりました日本原子力研究開発機構の皆様、三菱マテリアルの皆様、早稲田大学環境保全センターの皆様、同物性計測センターの皆様に心より感謝申し上げます。

研究室でご支援、ご助力下さいました多くの先輩方、同輩や後輩の皆様に深く感謝の意を表します。非常勤講師としてお世話になりました早稲田大学高等学院の先生方に感謝申し上げます。

また、本研究は、文部科学省グローバル COE プログラム「実践的化学知」より助成を受けましたことを報告致します。

最後に、私を暖かく見守って下さった両親と妻や親族に心より感謝致します。

2014 年 2 月

早稲田大学大学院　先進理工研究科　応用化学専攻

平沢研究室　張　亮

早稲田大学　博士（工学）　学位申請　研究業績書

氏 名　　張　亮　　印

（2014 年 1 月　現在）

種 類 別	題名、　発表・発行掲載誌名、　発表・発行年月、　連名者（申請者含む）
1. 論文	○Liang Zhang, Izumi Hirasawa: Evaluation of precipitation behavior of zirconium molybdate hydrate, Frontiers Chemical Science and Engineering, Vol.7 (1), 65-71 (2013) ○Liang Zhang, Izumi Hirasawa: Preventing zirconium molybdate accumulation based on crystallization, Chemical Engineering & Technology (accepted) ○Liang Zhang, Izumi Hirasawa: Research on shape-controled zirconium molybdate in the process of reaction crystallization, Journal of Chemical Engineering of Japan (accepted)
2. 講演	Liang Zhang, Izumi Hirasawa: Preventing zirconium molybdate accumulation based on crystallization, BIWIC2013, P-05, Odesen, Denmark, September 2013 Liang Zhang, Izumi Hirasawa: Evaluation of precipitation behavior of zirconium molybdate, BIWIC2012, P-12, Tianjin, China, July 2012 Liang Zhang, Izumi Hirasawa: Evaluation of precipitation behavior of zirconium molybdate, ACTS2012, SEO-O-12, Seoul, Korea, May 2012 Liang Zhang, Izumi Hirasawa: Evaluation of precipitation behavior of zirconium molybdate, The 6st Global COE International Symposium on Practical Chemical Wisdom, P-21, Tokyo, Japan, December 2011 池田匠輝, 張亮, 竹内正行, 小泉務, 平沢泉, 反応晶析過程におけるモリブデン酸ジルコニウムの形状および粒径評価, 分離技術会, S6-P144, 2013 年 5 月 池田匠輝, 張亮, 竹内正行, 小泉務, 平沢泉, 反応晶析過程におけるモリブデン酸ジルコニウムの形状および粒径評価, 化学工学会岡山大会, T115, 2013 年 9 月
3. 受賞	○The best poster presentation award, ACTS2012, Seoul, Korea, May 2012